CUT&Tag recovers up to half of ENCODE ChIP-seq peaks in modifications of H3K27

Di Hu[1,2*], Leyla Abbasova[1,2*], Brian M Schilder[1,2], Alexi Nott[1,2], Nathan G Skene[1,2+], Sarah J Marzi[1,2+#]

[1] UK Dementia Research Institute, Imperial College London, London, UK
[2] Department of Brain Sciences, Imperial College London, London, UK
[*] These authors contributed equally: Di Hu, Leyla Abbasova
[+] These authors are joint senior authors: Nathan G Skene, Sarah J Marzi
[#] Correspondence: s.marzi@imperial.ac.uk

Abstract

Techniques for genome-wide epigenetic profiling have been undergoing rapid development toward recovery of high quality data from bulk and single cell samples. DNA-protein interactions have traditionally been profiled via chromatin immunoprecipitation followed by next generation sequencing (ChIP-seq), which has become the current standard for studying histone modifications or transcription factor binding. Cleavage Under Targets & Tagmentation (CUT&Tag) is a promising new technique, which enables profiling of such interactions *in situ* at high sensitivity and is adaptable to single cell applications. However thorough evaluation and benchmarking against established ChIP-seq datasets are still lacking. Here we comprehensively benchmarked CUT&Tag for H3K27ac and H3K27me3 against published ChIP-seq profiles from ENCODE in K562 cells. Across a total of 30 new and 6 published CUT&Tag datasets we found that no experiment recovers more than 50% of known ENCODE peaks, regardless of the histone mark. We tested peak callers MACS2 and SEACR, identifying optimal peak calling parameters. Balancing both precision and recall of known ENCODE peaks, SEACR without retention of duplicates showed the best performance. We found that reducing PCR cycles during library preparation lowered duplication rates at the expense of ENCODE peak recovery. Despite the moderate ENCODE peak recovery, peaks identified by CUT&Tag represent the strongest ENCODE peaks and show the same functional and biological enrichments as ChIP-seq peaks identified by ENCODE. Our workflow systematically evaluates the merits of methodological adjustments, providing a benchmarking framework for the experimental design and analysis of CUT&Tag studies, and will facilitate future efforts to apply CUT&Tag in human tissues and single cells.

Keywords

Epigenomics, histone modifications, CUT&Tag, ChIP-seq, NGS, ENCODE

Background

In recent years the field of epigenetics has attracted increasing interest as a source of new insights into the mechanisms underlying human disease. Human disease risk variants identified through genome-wide association studies (GWAS) overwhelmingly localize to non-coding regions of the genome[1–3]. These risk variants appear to be enriched in gene regulatory regions. Chromatin dynamics at regulatory regions are governed by nucleosomes and their post-translational modifications, as well as interacting chromatin-associated complexes and transcription factors. Chromatin marks can define regions of activation and silencing, and mark transcriptional regulatory elements. These can be cell type-specific and are known to be dynamic during the course of embryonic development, aging, and disease progression[4]. Disease risk variants appear to be specifically enriched in active regulatory elements, particularly those marked by H3K27ac [5,6]. H3K27ac is a highly cell type specific histone modification and a marker of active enhancers and promoters[7] which has been implicated in complex diseases. For example, in the brain, variation in H3K27ac has been associated with neurodegenerative and neuropsychiatric disorders, including Alzheimer's disease[5,8,9]. However, understanding the precise regulatory mechanisms underlying epigenetic regulation in complex human disease and linking non-coding variants to disease phenotypes has been impeded by a lack of epigenomic annotations in disease and control tissues. Furthermore, the resources that do exist tend to use bulk tissues of heterogeneous organs, which is predominantly influenced by cell type composition and obscures cell type specific regulatory landscapes.

For many years, chromatin immunoprecipitation followed by next generation sequencing (ChIP-seq) has served as a standard method for epigenomic profiling. In ChIP-seq, chromatin is first cross-linked and solubilized, after which a primary antibody specific for the histone mark of interest enables immunoprecipitation of bound DNA[10]. However, it has potential limitations, such as low signal-to-noise ratio, epitope masking from fixation and cross-linking, and heterochromatin bias from chromatin sonication[11,12]. ChIP-seq poses challenges when working with low cell numbers, requiring approximately 1-10 million cells as input, with high demands on sequencing coverage, due to the low signal-to-noise ratio. In addition, ChIP-seq does not adapt well to single-cell applications due to its high cell input requirements and poor signal specificity. Cleavage Under Targets & Tagmentation (CUT&Tag) is a novel enzyme-tethering approach that has been presented as a streamlined, easily scalable, and cost-effective alternative to ChIP-seq. CUT&Tag has been reported to have superior chromatin mapping capabilities as compared to ChIP-seq at approximately 200-fold reduced cellular input and 10-fold reduced sequencing depth requirements[13]. CUT&Tag uses permeabilized nuclei to allow antibodies to bind chromatin associated factors, which enables tethering of protein A-Tn5 transposase fusion protein (pA-Tn5). Upon activation of pA-Tn5, cleavage of intact DNA and insertion of adapters (tagmentation) occurs for paired-end DNA sequencing. Following tagmentation, DNA fragments remain inside the nucleus making the method amenable to single cell chromatin profiling applications, for example enabling individual sorting of nuclei and PCR barcoding. The increased signal-to-noise ratio of CUT&Tag for histone marks is attributed to the direct antibody tethering of pA-Tn5 and

its integration of adapters *in situ* while it stays bound to the antibody target of interest during incubation. The process involves minimal sample loss with direct enzymatic end-polishing and ligation compared to regular library preparation protocols that result in sample loss, e.g. in ChIP-seq and CUT&RUN[13].

For ChIP-seq, experimental and analytical guidelines as well as datasets generated by the Encyclopedia of DNA Elements (ENCODE) consortium have served as a standard reference panel to the field for years[14]. In contrast, as a relatively new method, CUT&Tag lacks equivalent systematic optimization or benchmarking against existing datasets and there is little established consensus regarding experimental recommendations and data analysis workflows. Here we undertook experimental optimizations and systematic benchmarking of CUT&Tag against ENCODE in human K562 cells for histone modifications H3K27ac and H3K27me3 to serve as a guide for the design and analysis of future CUT&Tag studies. Since the development of CUT&Tag has primarily assessed methyl marks, where H3K27me3 is the recommended positive control[15], we focused in-depth on underexplored H3K27ac, testing multiple ChIP-grade antibody sources[5,8,16,17], antibody dilutions, histone deacetylase inhibitors (HDACi), as well as PCR parameters, and DNA extraction methods for library preparation (**Fig. 1a**). Experimental outcomes were evaluated by quantitative polymerase chain reaction (qPCR) and paired-end genomic sequencing. Our computational workflow served to iteratively guide experimental optimizations, appraise CUT&Tag data quality, and benchmark CUT&Tag performance against ENCODE ChIP-seq profiles (**Fig. 1b**). We explored the suitability of different peak calling approaches (SEACR and MACS2), and the effects of inclusion versus exclusion of duplicate reads. We characterized the similarities and differences between CUT&Tag and ENCODE based on parameters including read- and peak-level correlation, regulatory element annotation, gene ontology enrichment, and transcription factor binding motif (TFBM) analysis. We provide a benchmarking pipeline EpiCompare[18] to help researchers optimally analyze and interpret CUT&Tag studies.

Results

Overview of systematic H3K27 CUT&Tag experimental design and analysis

To benchmark the performance of CUT&Tag against established ENCODE ChIP-seq, we profiled histone modifications H3K27ac, a marker of active enhancers and promoters, and H3K27me3, associated with heterochromatin and assessed in the original series of papers introducing CUT&Tag[13,15,19]. Both histone modifications were characterized in K562 cells, generating a total of 30 new CUT&Tag sequencing datasets. We undertook systematic experimental optimizations for H3K27ac CUT&Tag testing multiple ChIP-grade antibody sources[5,8,16,17], antibody dilutions (1:50, 1:100, 1:200), as well as different PCR cycle numbers, DNA extraction methods for library preparation, and histone deacetylase inhibitors (HDACi) (**Fig. 1a**). Primary conditions were first

validated by performing qPCR using positive and negative control primers designed based on ENCODE ChIP-seq peaks (**Table 1**). The best conditions were subsequently subjected to paired-end sequencing. Our computational workflow iteratively guided experimental optimizations, assessed data quality, and benchmarked CUT&Tag performance against ENCODE ChIP-seq (**Fig. 1b**).

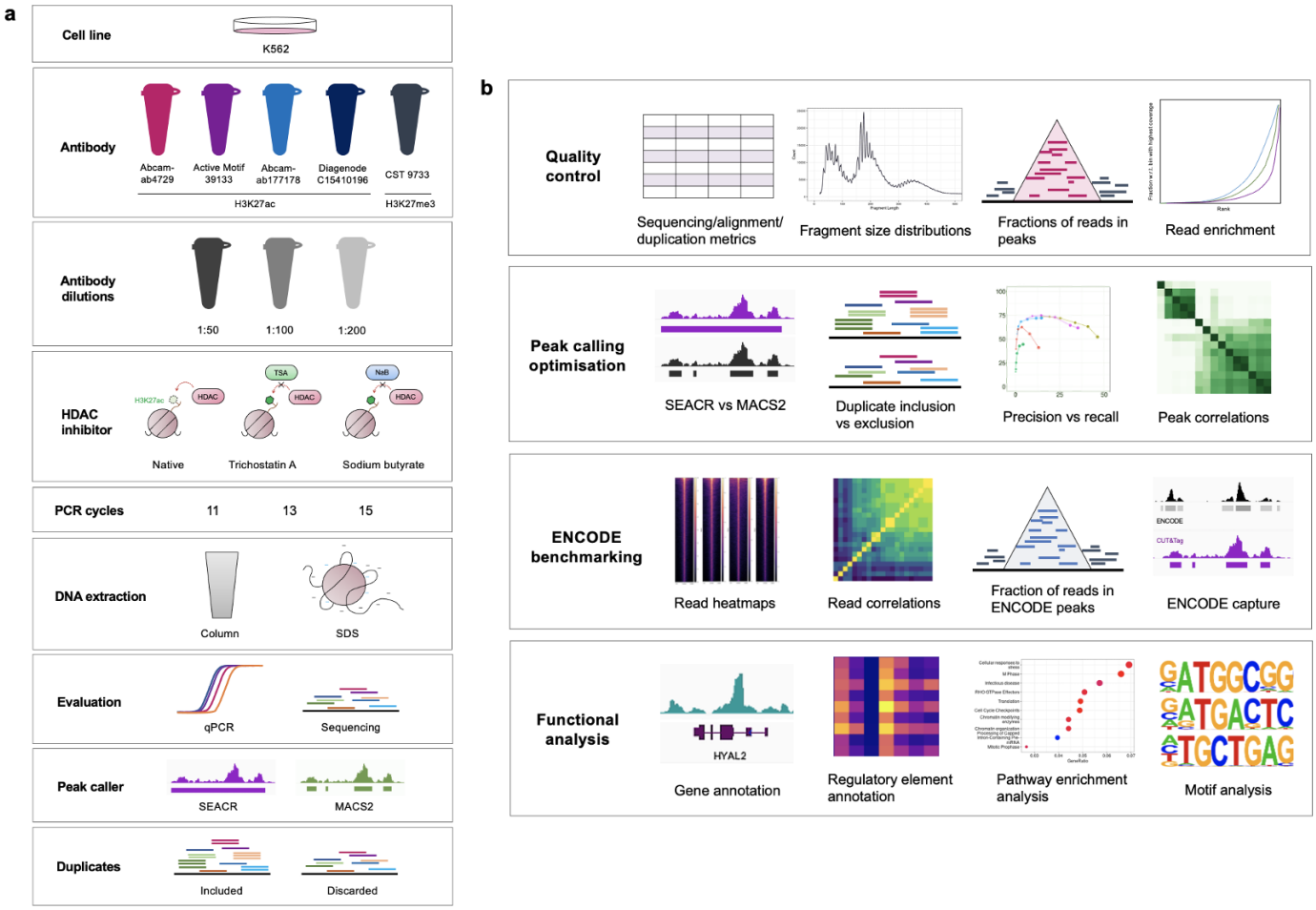

Figure 1. Overview of experimental design and computational benchmarking. a, Summary of experimental design: Five antibodies were tested at dilutions 1:50, 1:100 and 1:200, and 11, 13, or 15 PCR cycles for library preparation. H3K27ac libraries were assessed with and without HDAC inhibitor Trichostatin A (TSA; 1 μM), or sodium butyrate (NaB; 5 mM). Column- and SDS-based DNA extraction methods were compared. Antibody performance was assessed by qPCR and sequencing, and sequenced reads were processed with and without duplicates using peak callers SEACR and MACS2. **b**, Summary of analytical approaches: Analysis comprised quality control of sequencing data, optimization of peak calling approaches with both peak callers, and comparison between CUT&Tag and ENCODE datasets at the level of reads, peaks, and functional annotation.

Experimental optimisation of CUT&Tag

We first assessed four ChIP-seq grade H3K27ac antibodies across three dilutions (1:50, 1:100 and 1:200) by qPCR, using primers designed to amplify regions corresponding to genes falling into the most significant ENCODE peaks (positive controls: *ARGHAP22*, *COX4I2*, *MTHFR*, *ZMYND8*) versus least significant ENCODE peaks (negative controls: *KLHL11*, *SIGIRR*) (**Methods**; **Table 1**; **Fig. 2a**). Based on the outcome, we selected Abcam-ab4729 (1:100; the same antibody was used in ENCODE), Diagenode C15410196 (1:50 and 1:100), Abcam-ab177178 (1:100), and Active Motif 39133 (1:100) for sequencing. These antibodies will be henceforth referred to as Abcam-ab4729, Diagenode, Abcam-ab177178, and Active Motif. H3K27me3 CUT&Tag was profiled using ChIP-grade antibody Cell Signaling Technology-9733, the same antibody used in ENCODE, at dilution 1:100 as previously recommended[15]. In house samples were compared with published CUT&Tag[15] and CUT&RUN[20] data from the research group who originally developed these methods.

Since H3K27ac is dynamically deposited and removed by histone acetyltransferases and deacetylases (HDACs), chromatin mapping methods can potentially benefit from adding HDAC inhibitors (HDACi) to eliminate residual deacetylase activity and thereby stabilize acetyl marks. This is particularly relevant for CUT&Tag, which is carried out under native conditions where residual HDAC activity may have a greater impact. To test whether the addition of a potent HDAC inhibitor improves data quality and ENCODE coverage of previously tested antibodies, H3K27ac CUT&Tag was performed with addition of Trichostatin A (TSA; 1 μM). This data was compared to original samples scaled to the same read depths. Addition of TSA did not consistently increase total peak detection using SEACR with stringent settings and a threshold of 0.01 (**Supplementary Fig. 1a**), and improved neither signal to noise ratio (**Supplementary Fig. 1b**) nor ENCODE capture (**Fig. 2b**). Here, ENCODE capture was assessed using two metrics: precision (the proportion of CUT&Tag peaks falling into ENCODE peaks of the same histone modification) and recall (the proportion of ENCODE peaks captured by CUT&Tag). H3K27ac CUT&Tag was also attempted with addition of sodium butyrate (NaB; 5mM) and libraries were evaluated by qPCR to find no improvement in CUT&Tag binding signal (**Supplementary Fig. 1c**).

Preliminary analysis of sequencing data revealed high duplication rates across all samples (min: 55.49%; max: 98.45%; mean: 82.25%; **Supplementary Table 1**). CUT&Tag library preparation was initially carried out with 15 PCR cycles, as per the original protocol[14]. To test whether this contributed to high numbers of duplicate reads we carried out CUT&Tag library preparation at 11 and 13 PCR cycles. In addition to varying cycle numbers, we also appraised SDS-based vs column-based methods of DNA extraction (see methods). All samples were analyzed at the original read depth (**Fig. 2c-e**) and also downsampled to the shared minimum read depth (2.6 million paired-end reads; **Supplementary Fig. 1d-f**) to compare duplication rates, total unique fragments, and ENCODE coverage. Varying PCR cycles while employing SDS-based DNA extraction produced mixed changes in duplication rate, whereas samples obtained with column-based extraction predominantly showed an increase in duplication rate from 11 to 13 PCR cycles (**Fig. 2c**). Overall, the greatest numbers of unique fragments were generated using

15 PCR cycles and SDS-based DNA extraction (**Fig. 2d**), although the difference was less significant after downsampling (**Supplementary Fig. 1e**). Almost all samples captured ENCODE peaks with high precision regardless of condition and analysis approach, but total ENCODE recall by Abcam-ab4729 and Diagenode (1:50) was improved when using 15 PCR cycles (**Fig. 2e**). The superior unique fragment yield at 15 PCR cycles did not translate into improved ENCODE coverage after downsampling (**Supplementary Fig. 1f**). Based on these optimizations the 15 PCR cycle, SDS-based DNA extraction experiments without addition of HDACi were taken forward for systematic benchmarking.

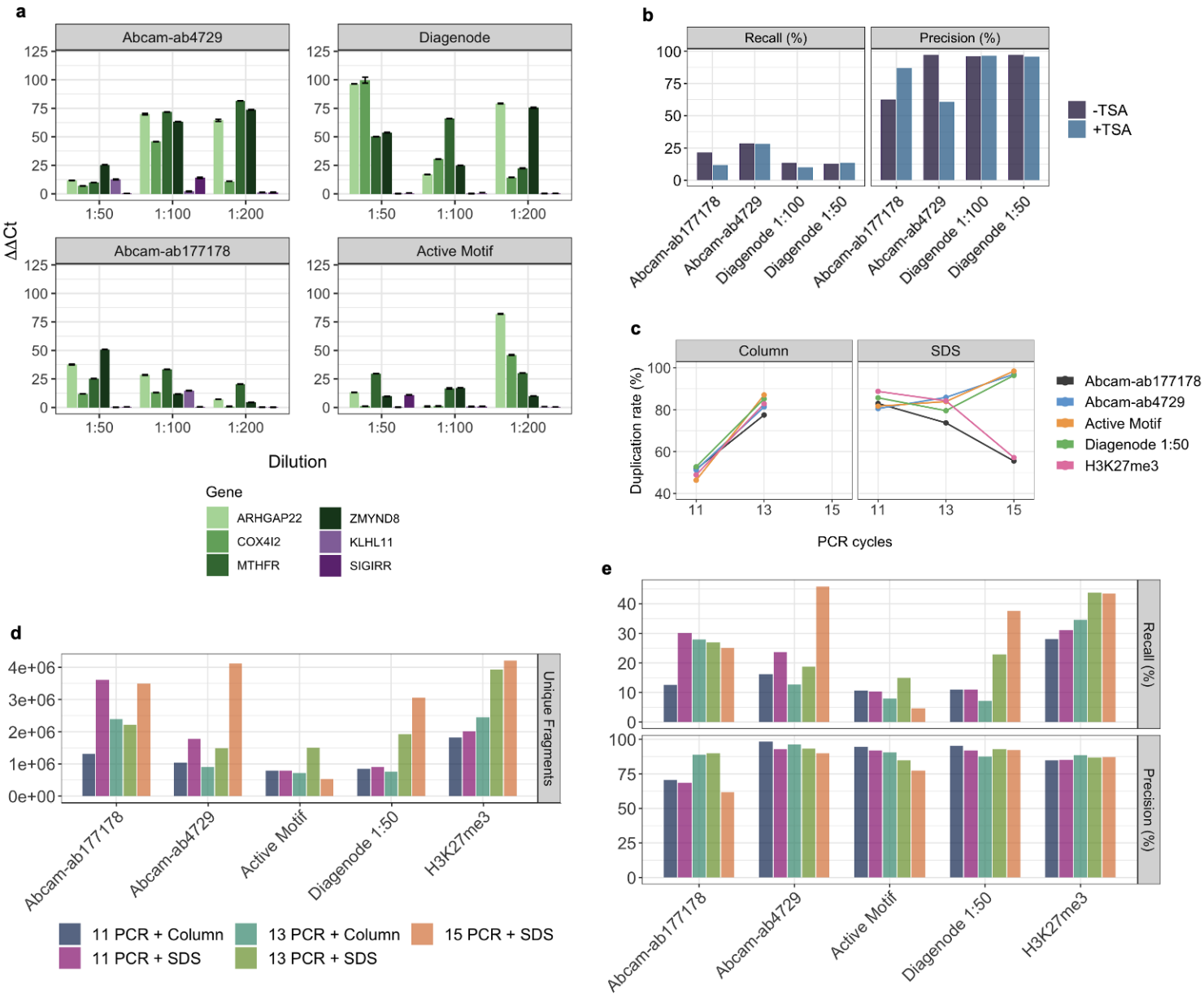

Figure 2. Experimental optimization of CUT&Tag. a, Results of qPCR amplification of genes falling into most significant ENCODE H3K27ac peak regions in CUT&Tag samples; **b**, Precision and recall of ENCODE H3K27ac peak capture with and without addition of HDAC inhibitor TSA. Reads from each antibody tested without TSA were downsampled to the same read depth as the same antibody tested with TSA. **c**, Duplication rates, **d**, total unique fragments, and **e**, ENCODE capture metrics obtained using column- or SDS-based DNA extraction and 11, 13 or 15 PCR cycles for sequencing library preparation, at the original read depth.

Quality control of CUT&Tag data

We first quantified fragment length to observe fragment sizes comparable to CUT&Tag in human nuclei, with an abundance of fragments at around 180bp in size, reflecting the length of DNA from a single nucleosome (**Fig. 3a; Supplementary Fig. 2a**)[21,22]. We also observed short fragments (<100bp) similar to previous CUT&Tag data[15], potentially caused by tagmentation of open chromatin[23]. Shorter fragments were not more abundant in duplicate-containing samples, suggesting that these are not a consequence of PCR amplification bias[24].

We next evaluated signal-to-noise quality by calculating the fractions of CUT&Tag reads in peaks (FRiPs) using peaks we defined with our dataset, as well as CUT&Tag reads in pre-defined ENCODE peaks. Specifically, we compared our data with ENCODE H3K27ac narrow and H3K27me3 broad peak sets (**Fig. 3b**). To identify peaks in our CUT&Tag data we used two analytical approaches: 1) MACS2, a standard peak caller for ChIP-seq data used by ENCODE and also applied to recent CUT&Tag datasets, and 2) SEACR, an algorithm developed specifically to detect peaks in high signal-to-noise data, such as CUT&RUN and CUT&Tag[25,26]. With few exceptions, the fractions of reads in CUT&Tag called peaks and ENCODE peaks of the same mark were comparable. Of the antibodies tested, Abcam-ab4729 and Diagenode at 1:50 dilution showed the highest percentage of reads falling into published ENCODE H3K27ac peaks (29.9% and 27.4%, respectively), as well as peaks identified in the CUT&Tag sample (SEACR: 35.3% and 32.9%, MACS: 34.1% and 30.9%, respectively; **Fig. 3b; Supplementary Fig. 2b**). However, all H3K27ac CUT&Tag FRiP scores were markedly lower than ENCODE H3K27ac ChIP-seq's own reported score of 42%. Only H3K27me3 CUT&Tag FRiPs in ENCODE peaks slightly outperformed ENCODE H3K27me3's FRiP score of 66%, but this was not reflected in the enrichment across empirically identified SEACR and MACS2 peaks (**Fig. 3b**). Of note, H3K27me3 CUT&Tag shows highly specific enrichment for ENCODE H3K27me3 peaks, while H3K27ac shows more unspecific enrichment at ENCODE H3K27ac and H3K27me3 peaks, both for in house and published data. Duplicate inclusion did not make a significant difference to peak calling except in cases where peaks of highly duplicated samples were called using MACS2. Visualization in the Integrative Genomics Viewer[27] showed variable noise levels for H3K27ac CUT&Tag relative to ENCODE ChIP-seq, while H3K27me3 CUT&Tag exhibited consistently lower background noise (**Fig. 3c**). To correct for potential differences in breadth and read capture of ENCODE and CUT&Tag peaks, FRiPs calculations were repeated using intersecting ENCODE and CUT&Tag peak regions, which were determined separately for each CUT&Tag sample (**Supplementary Fig. 2c**). This revealed that while H3K27ac FRiP scores were relatively similar for CUT&Tag and ENCODE, H3K27me3 CUT&Tag produced over twice as many reads in overlapping intervals than ENCODE.

Since CUT&Tag and other Tn5 transposase-based methods may be susceptible to open chromatin bias[28], we assessed the proportion of reads falling into open chromatin ATAC-seq peaks (**Fig. 3d; Supplementary Fig. 2d**). Nearly 70% of ENCODE H3K27ac peaks overlapped

with ATAC-seq peaks. Therefore ENCODE H3K27ac peaks were further subset to obtain those exclusive to the histone modification, exclusive to ATAC, and shared by both (**Fig. 3d**). This revealed that nearly all H3K27ac regions profiled by CUT&Tag fall into open chromatin regions shared with ATAC, but not into ATAC-only regions. For H3K27me3, around 8% of reads fell into ATAC peaks and this percentage was similar across comparison data. Removing short fragments (<100 bp) reduced the proportion of overlap with ATAC peaks to 4.6% for H3K27me3 (42.5% reduction), while short fragment exclusion had a negligible effect on H3K27ac/ATAC overlap.

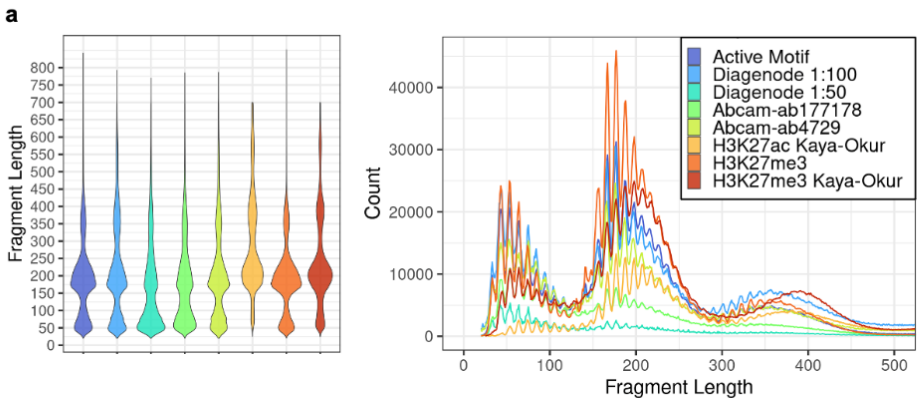
a
Fragment Length
Count
Fragment Length
Active Motif
Diagenode 1:100
Diagenode 1:50
Abcam-ab177178
Abcam-ab4729
H3K27ac Kaya-Okur
H3K27me3
H3K27me3 Kaya-Okur

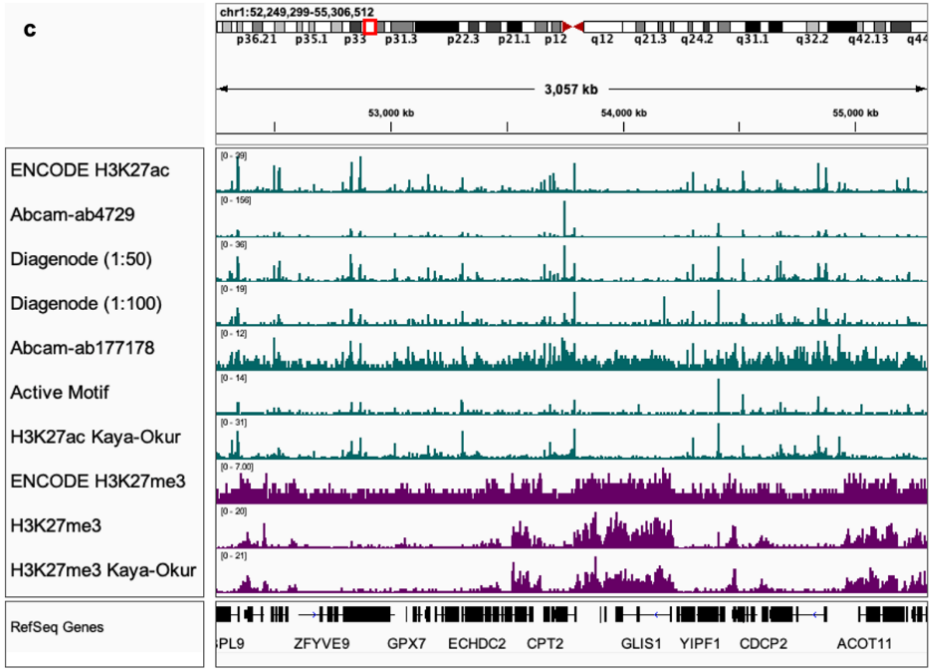
c
chr1:52,249,299-55,306,512
3,057 kb
53,000 kb
54,000 kb
55,000 kb
ENCODE H3K27ac
Abcam-ab4729
Diagenode (1:50)
Diagenode (1:100)
Abcam-ab177178
Active Motif
H3K27ac Kaya-Okur
ENCODE H3K27me3
H3K27me3
H3K27me3 Kaya-Okur
RefSeq Genes
ZFYVE9
GPX7
ECHDC2
CPT2
GLIS1
YIPF1
CDCP2
ACOT11

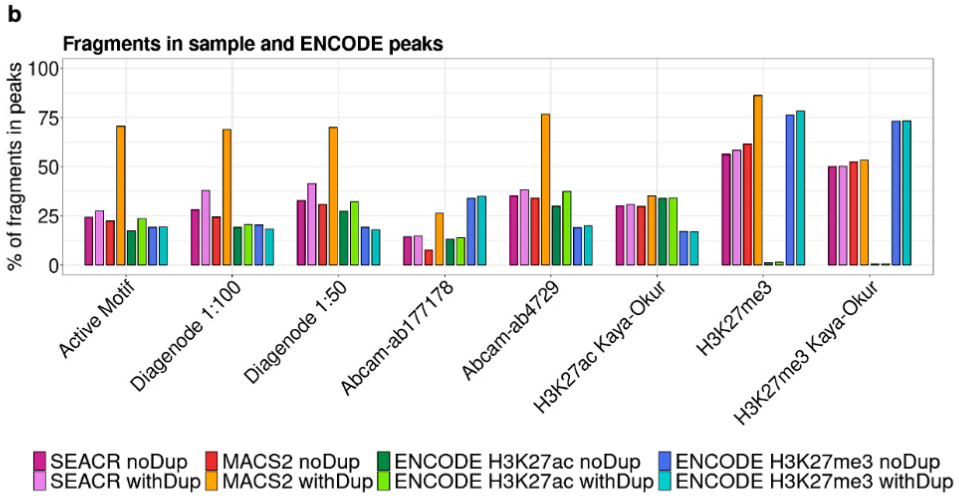
b
Fragments in sample and ENCODE peaks
% of fragments in peaks
Active Motif
Diagenode 1:100
Diagenode 1:50
Abcam-ab177178
Abcam-ab4729
H3K27ac Kaya-Okur
H3K27me3
H3K27me3 Kaya-Okur
SEACR noDup
SEACR withDup
MACS2 noDup
MACS2 withDup
ENCODE H3K27ac noDup
ENCODE H3K27ac withDup
ENCODE H3K27me3 noDup
ENCODE H3K27me3 withDup

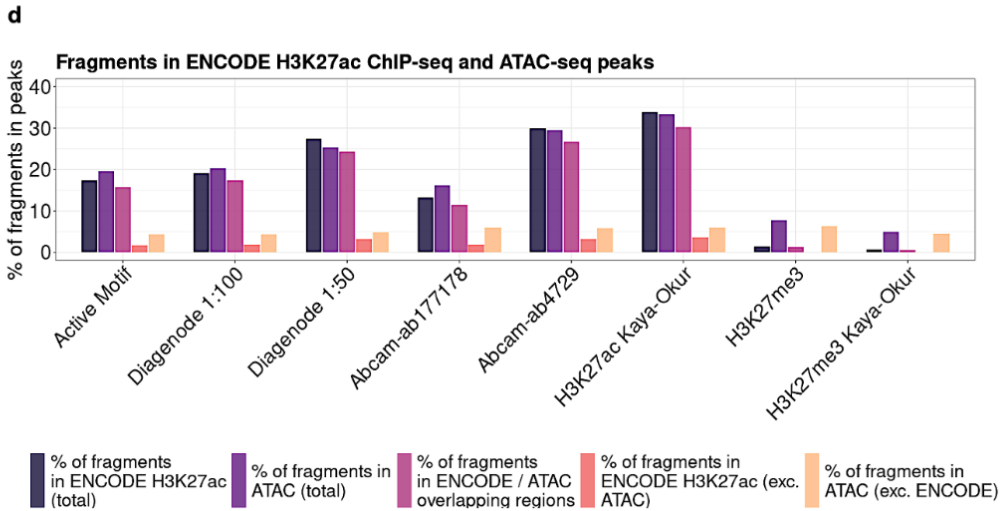
d
Fragments in ENCODE H3K27ac ChIP-seq and ATAC-seq peaks
% of fragments in peaks
Active Motif
Diagenode 1:100
Diagenode 1:50
Abcam-ab177178
Abcam-ab4729
H3K27ac Kaya-Okur
H3K27me3
H3K27me3 Kaya-Okur
% of fragments in ENCODE H3K27ac (total)
% of fragments in ATAC (total)
% of fragments in ENCODE / ATAC overlapping regions
% of fragments in ENCODE H3K27ac (exc. ATAC)
% of fragments in ATAC (exc. ENCODE)

Figure 3. Quality control metrics for CUT&Tag and comparison data. a, CUT&Tag fragment size distributions; **b**, Fractions of reads in peaks (FRiPs) called on each sample with SEACR and MACS2, as well as in ENCODE reference H3K27ac and H3K27me3 peaks; **c**, Integrative Genomics Viewer (IGV)[27] tracks showing sample read pileups; **d**, Fractions of sample reads in ENCODE H3K27ac ChIP-seq and ATAC-seq peaks.

CUT&Tag peak calling with SEACR and MACS2

We next assessed different peak callers and their settings to identify which would be most suitable for CUT&Tag. We evaluated the performance of both SEACR and MACS2, which were developed for CUT&RUN[26] and ChIP-seq[29], respectively. Parameter optimization was conducted based on precision and recall of ENCODE ChIP-seq peak capture by CUT&Tag (**Fig. 4a; Supplementary Fig. 3a-d**), with the aim of maximizing ENCODE capture while maintaining high precision (>80%). SEACR peaks were called using the stringent setting and thresholds of 0.01, 0.03, 0.05 and 0.1, as the relaxed setting was found to be too permissive, with precision scores consistently falling below the 80% threshold. MACS2 peaks were called using the narrow peak setting, with p- and q-values between $1x10^{-5}$ and 0.1. These settings were also tested with local lambda deactivated to replicate the global background approximation employed by SEACR. On the basis of precision and recall analysis, optimum SEACR H3K27ac peaks were called using the stringent setting and a threshold of 0.01. For MACS2, H3K27ac narrow peaks were called with local lambda deactivated and a q-value of $1x10^{-5}$. As a broader histone mark, H3K27me3 peaks were called with the same settings, but using the broad flag in MACS2, or by increasing the SEACR threshold to 0.1. Based on these parameters, SEACR peaks were called with slightly higher precision compared to MACS2 (**Fig. 4a**). Peak calling was also attempted using above mentioned parameters and published IgG control data, but this did not improve ENCODE capture (**Supplementary Fig. 3e**). Therefore, a control was not used for further analyses. While levels of noise in H3K27ac samples were variable and elevated relative to ENCODE, H3K27me3 CUT&Tag showed lower background compared to both H3K27ac CUT&Tag and H3K27me3 ChIP-seq. CUT&Tag peaks identified with both peak callers appeared to miss some ENCODE peaks of lower signal intensity, particularly in regions of elevated background noise. (**Fig. 4b; Supplementary Fig. 3f**). While SEACR peak calling was largely unaffected by duplicate inclusion, MACS2 showed very high duplicate sensitivity, identifying an excessive number of spurious peaks despite stringent parameters (**Supplementary Table 2**). Furthermore, SEACR defined wider peaks than MACS2, where multiple MACS2 peaks corresponded to a single SEACR peak (**Fig. 4b; Supplementary Fig. 3f**). While this may not pose an issue for broader histone marks, such as H3K27me3, it may complicate detection of subtle, local changes in histone modifications, and potentially merge nearby promoter and enhancer peaks. Comparing the widths of all sample peaks, and only those peaks falling within 1.5kb up- or downstream of promoter regions, confirmed that SEACR detects significantly broader H3K27ac peaks than MACS2, whereas for the H3K27me3 mark both callers performed comparably (**Supplementary Fig. 3g**). To test whether these promoter-overlapping peaks are more likely to capture

enhancers, we used published STARR-seq data[30] (see **Methods**). STARR-seq peaks were filtered to retain those that fall into K562 DNase-seq regions to yield putative cell-specific enhancers. Calculating enhancer capture did not reveal a significant difference in promoter-enhancer co-occurrence among SEACR and MACS2 promoter-containing peaks (**Supplementary Fig. 3h**). Furthermore, both peak callers showed a near 1:1 ratio of sample peaks to captured promoter regions (**Supplementary Fig. 3i**). Peak correlations, quantified with DiffBind[31], revealed that SEACR calls peaks with higher consistency than MACS2, whereas MACS2 CUT&Tag peaks show greater similarity to ENCODE peaks, which are also called using MACS2 (**Fig. 4c**). Following subsampling to the same read depths, read profiles around peak summits confirmed that at the selected settings, peaks called by SEACR and MACS2 possessed similar read densities (**Fig. 4d**). Furthermore, the best-performing CUT&Tag samples showed greater peak read enrichment compared to ENCODE. However, this does not necessarily translate to higher FRiPs, which depend on abundance of reads, a metric not incorporated into peaks.

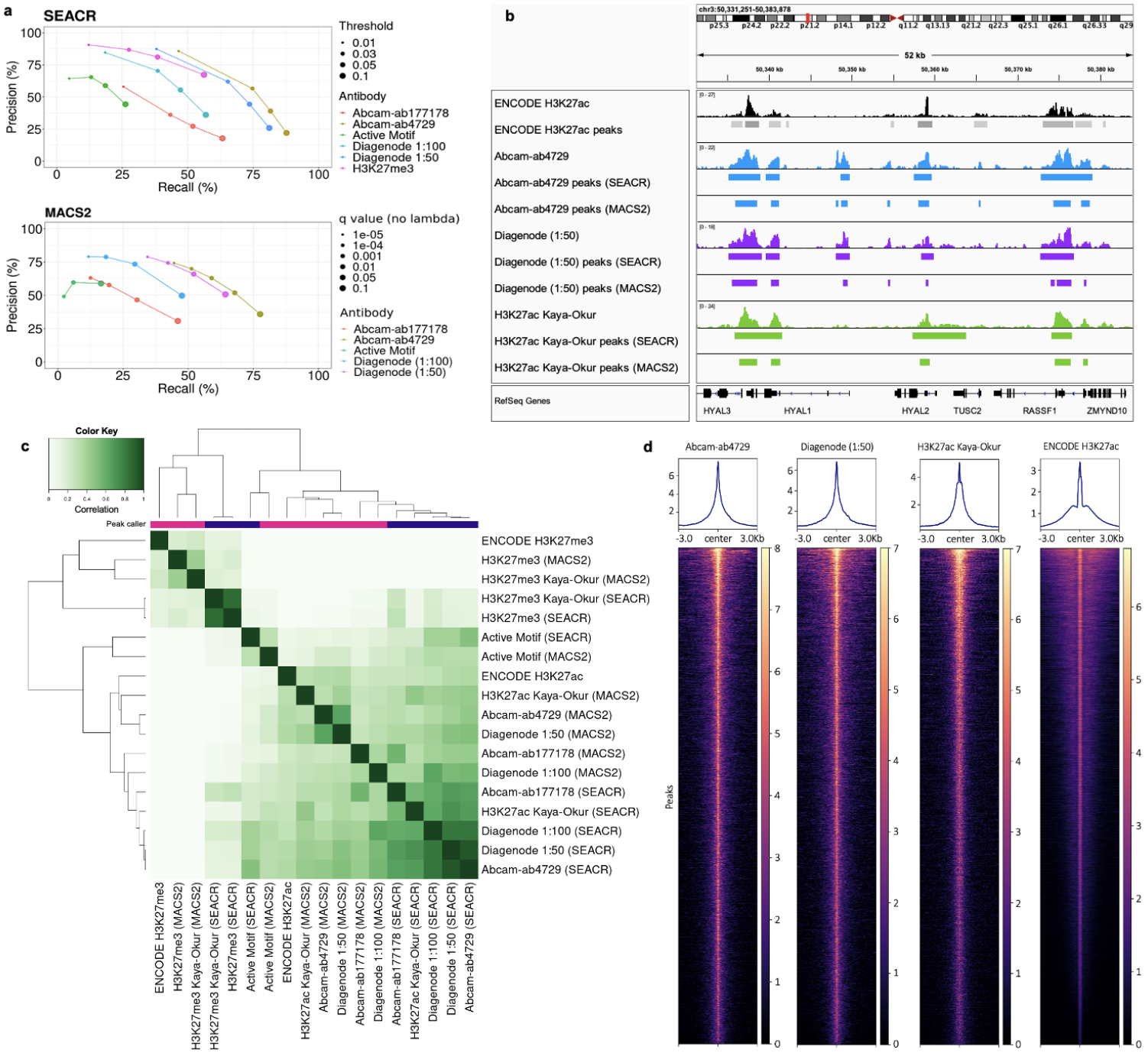
a
SEACR
Precision (%)
Recall (%)
Threshold
0.01
0.03
0.05
0.1
Antibody
Abcam-ab177178
Abcam-ab4729
Active Motif
Diagenode 1:100
Diagenode 1:50
H3K27me3
MACS2
q value (no lambda)
1e-05
1e-04
0.001
0.01
0.05
0.1
Antibody
Abcam-ab177178
Abcam-ab4729
Active Motif
Diagenode (1:100)
Diagenode (1:50)
b
chr3:50,331,251-50,383,878
52 kb
ENCODE H3K27ac
ENCODE H3K27ac peaks
Abcam-ab4729
Abcam-ab4729 peaks (SEACR)
Abcam-ab4729 peaks (MACS2)
Diagenode (1:50)
Diagenode (1:50) peaks (SEACR)
Diagenode (1:50) peaks (MACS2)
H3K27ac Kaya-Okur
H3K27ac Kaya-Okur peaks (SEACR)
H3K27ac Kaya-Okur peaks (MACS2)
RefSeq Genes
HYAL3
HYAL1
HYAL2
TUSC2
RASSF1
ZMYND10
c
Color Key
Correlation
Peak caller
ENCODE H3K27me3
H3K27me3 (MACS2)
H3K27me3 Kaya-Okur (MACS2)
H3K27me3 Kaya-Okur (SEACR)
H3K27me3 (SEACR)
Active Motif (SEACR)
Active Motif (MACS2)
ENCODE H3K27ac
H3K27ac Kaya-Okur (MACS2)
Abcam-ab4729 (MACS2)
Diagenode 1:50 (MACS2)
Abcam-ab177178 (MACS2)
Diagenode 1:100 (MACS2)
Abcam-ab177178 (SEACR)
H3K27ac Kaya-Okur (SEACR)
Diagenode 1:100 (SEACR)
Diagenode 1:50 (SEACR)
Abcam-ab4729 (SEACR)
d
Abcam-ab4729
Diagenode (1:50)
H3K27ac Kaya-Okur
ENCODE H3K27ac
-3.0 center 3.0Kb
Peaks

Figure 4. Peak calling with SEACR and MACS2. a, Panel showing precision/recall plots for SEACR and one of several MACS2 tests employed with different parameters; **b**, Select H3K27ac sample tracks visualized using the IGV, alongside called SEACR and MACS2 peak ranges; **c**, Correlations between sample peaks called with both peak callers (pink corresponds to MACS2, and blue corresponds to SEACR peaks); **d**, Average read enrichments around summits of select peaks called with SEACR and ENCODE H3K27ac, all subsampled to 2 million reads.

Benchmarking of CUT&Tag against ENCODE ChIP-seq

We next proceeded to benchmark CUT&Tag against ENCODE ChIP-seq profiles. First, in an attempt to minimize any bias potentially incurred by peak calling, samples were correlated on the basis of read counts in different genomic regions: ENCODE H3K27ac peak ranges (**Fig. 5a; Supplementary Fig. 4a**), the hg19 reference genome[32] partitioned into 500bp bins (**Supplementary Fig. 4b**), and ENCODE H3K27me3 peak ranges (**Supplementary Fig. 4c**). While genome-wide correlation revealed that similarity between CUT&Tag (and CUT&RUN) samples was markedly higher than that between CUT&Tag and ENCODE ChIP-seq, CUT&Tag-ENCODE correlations were much enhanced when the analysis was restricted to ENCODE H3K27ac and H3K27me3 peak regions for the corresponding mark. This is likely because genome-wide comparison factors in many regions that are devoid of true signal or contain noise, adding unwanted variability to the correlation analysis. On the whole, there was good correspondence between read- (**Fig. 5a**) and peak-level (**Fig. 4c**) correlations. To determine the extent to which CUT&Tag recovers known ChIP-seq peaks, the GenomicRanges[33] package was used to calculate the proportion of ENCODE peaks overlapping with CUT&Tag (recall), and the proportion of sample peaks overlapping with ENCODE (precision; **Fig. 5b; Supplementary Fig. 4d**). Overall, MACS2 achieved slightly higher recall at the expense of precision, which could be matched by marginally raising the SEACR threshold. The maximum ENCODE capture for H3K27ac was approximately 45% attained using the best-performing antibody Abcam-ab4729. This empirical ceiling was also observed across the comparison of previously published H3K27ac CUT&Tag and CUT&RUN samples (**Supplementary Fig. 4d**). Despite the much greater number of peaks called, H3K27me3 CUT&Tag only reached an ENCODE coverage ceiling of approximately 50%, recovering up to half of ENCODE ChIP-seq peaks. To test whether these metrics might be improved by further increasing library complexity, we generated aggregate, merged samples comprising either all internal CUT&Tag samples, or all internal and published CUT&Tag samples used in this study. Calculating precision and recall at different SEACR thresholds showed that at 80% precision, these samples recovered 59.6% and 64.2.% of ENCODE peaks, respectively (**Supplementary Fig. 4e**). To see whether these conclusions might hold true for other cell types, we also assessed ENCODE precision and recall using published H3K27me3 CUT&Tag data from the HCT116 cell line[34] to find even poorer ENCODE capture at comparable levels of precision (**Supplementary Fig. 4f**).

To facilitate comparison between different samples, precision and recall were compounded into a single metric representing a weighted average of the two measures, the F1-score (**Methods**; **Supplementary Fig. 4g**). This approach excludes true negative peaks, which might distort the score since they occupy the vast majority of the genome. We confirmed Abcam-ab4729 as the best performing antibody, followed by Diagenode at 1:50 dilution, while also highlighting that peak calling with SEACR resulted in better F1-scores than MACS2 on average (**Supplementary Fig. 4g**). For antibody selection, ENCODE coverage was re-calculated with all samples subsampled to the same read depth. This confirmed that Abcam-ab4729 still outperformed other tested antibodies (**Supplementary Fig. 4h**). Duplicates in CUT&Tag data may have biological relevance, potentially arising from tagmentation events that recur in the same place by chance. Thus, peaks were called with versus without duplicates. Duplicate inclusion in samples with relatively low duplication rates had little to no effect on precision or recall; however, in samples more abundant in duplicates, peak calling with duplicates using MACS2 was compromised by detection of abundant spurious peaks (**Fig. 5b**). Any improvements seen for ENCODE recall came at the expense of detection of a large number of false positive peaks. We thus recommend exclusion of duplicates.

To further characterize the ENCODE H3K27ac peaks that were captured and missed by each CUT&Tag sample, the -log(q) values (significance) of the ENCODE peaks (from original peak calling performed in ENCODE) were compared, showing that CUT&Tag captures the most significant peaks (**Fig. 5c**). We supplemented this by analyzing ATAC-seq read counts (**Fig. 5d**), as in principle the H3K27ac mark should coincide with open chromatin regions. This showed that the ENCODE peaks captured by CUT&Tag samples contain more ATAC reads even when corrected for total base count of the captured and missed ENCODE peak sets, supporting the notion that CUT&Tag detects more prominent H3K27ac peaks, or at least those that are more likely to also be detected by an orthogonal epigenomic method. In all cases the differences between the q-values and ATAC-seq read counts in captured and missed ENCODE peaks were statistically significant ($p<0.0001$ across all q-value pairs and $p=0.0002$ for ATAC reads, respectively; two-tailed t-test). Due to lower background, CUT&Tag should allow for higher data quality at read depths lower than those required for ChIP-seq, as previously shown for methyl histone marks[15]. To test whether H3K27ac CUT&Tag might have an advantage at lower read depths, FRiPs were calculated at 0.5, 1, 1.5 and 2 million unique reads (**Fig. 5e**). This analysis showed that the best H3K27ac CUT&Tag antibodies still produced fewer reads in peaks than ENCODE ChIP-seq at low read depth, although CUT&Tag peaks showed greater read enrichment around peak summits compared to ChIP-seq peaks (**Fig. 5f**). Cumulative sample read enrichments at equal read depths revealed that the read distributions of H3K27ac CUT&Tag and H3K27ac ENCODE ChIP-seq samples were comparable, while H3K27me3 CUT&Tag samples showed more constrained read distributions than ENCODE H3K27me3 (**Fig. 5g**). In agreement with the FRiPs analyses, this indicates that even at equal read depths, H3K27ac – but not H3K27me3 – CUT&Tag samples contain more off-target reads than ENCODE ChIP-seq.

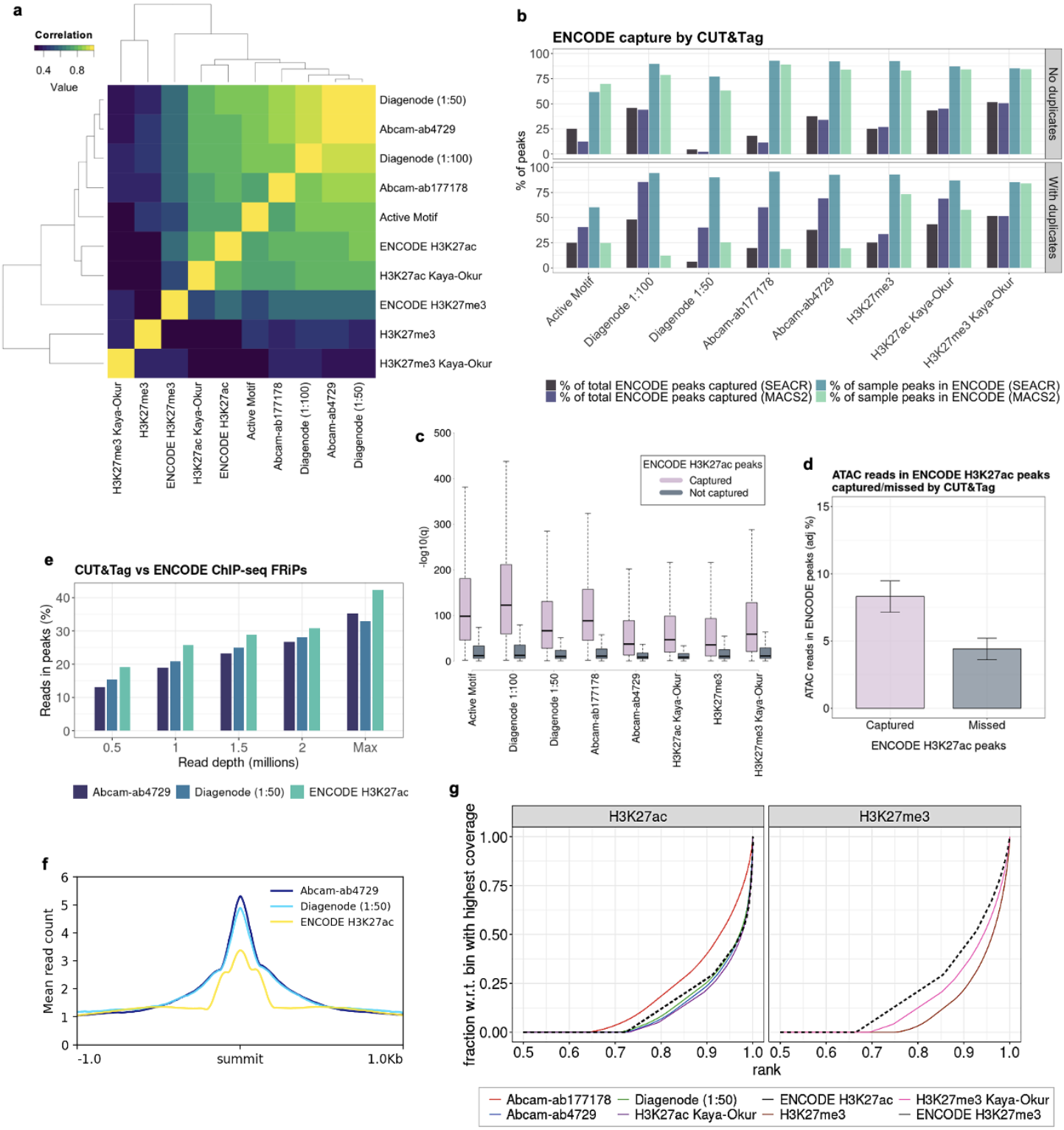
a
Correlation
0.4 0.8
Value
Diagenode (1:50)
Abcam-ab4729
Diagenode (1:100)
Abcam-ab177178
Active Motif
ENCODE H3K27ac
H3K27ac Kaya-Okur
ENCODE H3K27me3
H3K27me3
H3K27me3 Kaya-Okur
b
ENCODE capture by CUT&Tag
% of peaks
No duplicates
With duplicates
Active Motif
Diagenode 1:100
Diagenode 1:50
Abcam-ab177178
Abcam-ab4729
H3K27me3
H3K27ac Kaya-Okur
H3K27me3 Kaya-Okur
% of total ENCODE peaks captured (SEACR)
% of total ENCODE peaks captured (MACS2)
% of sample peaks in ENCODE (SEACR)
% of sample peaks in ENCODE (MACS2)
c
ENCODE H3K27ac peaks
Captured
Not captured
-log10(q)
d
ATAC reads in ENCODE H3K27ac peaks captured/missed by CUT&Tag
ATAC reads in ENCODE peaks (adj %)
Captured
Missed
ENCODE H3K27ac peaks
e
CUT&Tag vs ENCODE ChIP-seq FRiPs
Reads in peaks (%)
Read depth (millions)
Max
Abcam-ab4729
Diagenode (1:50)
ENCODE H3K27ac
f
Mean read count
Abcam-ab4729
Diagenode (1:50)
ENCODE H3K27ac
-1.0
summit
1.0Kb
g
H3K27ac
H3K27me3
fraction w.r.t. bin with highest coverage
rank
Abcam-ab177178
Abcam-ab4729
Diagenode (1:50)
H3K27ac Kaya-Okur
ENCODE H3K27ac
H3K27me3
H3K27me3 Kaya-Okur
ENCODE H3K27me3

Figure 5. Benchmarking of CUT&Tag against ENCODE. a, Correlation of sample read counts across ENCODE H3K27ac peak ranges; **b**, Percentages of CUT&Tag peaks falling into ENCODE H3K27ac, and of ENCODE H3K27ac peaks captured by CUT&Tag, with and without duplicates; **c**, Comparison of $-\log_{10}(q)$ values of ENCODE H3K27ac peaks captured and not captured by CUT&Tag; boxplot whiskers correspond to 1.5 * the interquartile range (IQR); **d**, Measures of relative abundance of ATAC-seq reads in ENCODE H3K27ac peaks captured and not captured by CUT&Tag; bars correspond to the standard deviation; **e**, FRiPs of select top H3K27ac CUT&Tag sample peaks and ENCODE H3K27ac peaks at different read depths, and at the original sequencing depth ('Max'); **f**, Average read counts around MACS2 peak summits of top H3K27ac CUT&Tag samples and ENCODE ChIP-seq peaks; **g**, Fingerprint plots of H3K27ac (left) and H3K27me3 (right) CUT&Tag and ENCODE, all subsampled to 2 million reads. Dashed lines indicate ENCODE samples. The bin with the highest coverage refers to the 1000bp interval containing the most reads; graphs show the cumulative read counts within ranked 1000bp bins, as a fraction of the read count in the highest-scoring bin.

Functional analysis of CUT&Tag peaks

To investigate functional similarities of peaks identified by CUT&Tag compared to ENCODE ChIP-seq, we assessed the genomic distribution of CUT&Tag peaks in relation to genes and chromatin states. Using ChIPseeker, peaks were annotated with and mapped in relation to their proximal genes. This revealed a strong skew towards promoter proximal regions for H3K27ac CUT&Tag samples, and a corresponding depletion in promoter regions for H3K27me3 (**Fig. 6a**). H3K27ac CUT&Tag exhibited a stronger promoter preference than H3K27ac ENCODE ChIP-seq, particularly for peaks called by SEACR (**Supplementary Fig. 5a**). H3K27ac CUT&Tag also showed enrichments for distal intergenic regions, which likely harbor a significant fraction of enhancers[35]. Next we explored an alternative gene-independent breakdown of functional genomic elements by assigning peaks to ChromHMM-derived chromatin states[36] using the genomation R package[37]. This confirmed a predominance of promoters and enhancers amongst the regions mapped by H3K27ac CUT&Tag (**Fig. 6b; Supplementary Fig. 5b**). In contrast, H3K27me3 overwhelmingly localized to heterochromatic and repressed chromatin regions, as would be expected. The two peak callers showed slight differences in regulatory element enrichment. While MACS2 corresponded better to ENCODE H3K27ac, SEACR peaks were more enriched at weak enhancers, weak promoters, weakly transcribed regions, and regions of transcriptional transition from initiation to elongation than their MACS2-called counterparts (**Fig. 6b**). This could be in part attributed to the fact that SEACR peaks are broader than MACS2 peaks and thus more likely to extend to neighboring elements.

Peaks specific to duplicate-containing samples were functionally annotated to reveal that a significant portion of excess MACS2 peaks called upon inclusion of duplicates fall into heterochromatic regions, even among H3K27ac CUT&Tag samples (**Supplementary Fig. 5c**).

This suggests that duplicates should not be retained when calling peaks with MACS2, as it can lead to artifacts. On the other hand, the few extra peaks called by including duplicates in SEACR match the regulatory element distribution of the corresponding deduplicated peaks. Finally, CUT&Tag peaks that did not overlap with ENCODE spanned diverse element types, with tested antibodies showing an enrichment in areas of weak transcription, weak enhancers and heterochromatin, while published CUT&Tag and CUT&RUN data showed an enrichment for transcription elongation, weak transcription, weak enhancer and transcription transition categories (**Supplementary Fig. 5d**). For H3K27me3, these peaks were still almost exclusively located in heterochromatic regions. Read distributions around transcription start sites (TSS) obtained from NCBI RefSeq[38] were visualized with heatmaps, which showed enrichment around TSS for H3K27ac (**Supplementary Fig. 5e**). Although CUT&Tag was found to capture slightly fewer promoters overall compared to ChIP-seq when subsampled to the same read depth (not shown), it showed higher average read densities in these regions for H3K27ac (**Supplementary Fig. 5e**). Reads from H3K27me3 samples did not co-localize with promoters.

Enhancer enrichment was further tested by measuring capture of genome-wide STARR-seq peaks[30], at baseline and controlling for total genomic coverage (8Mb). ENCODE H3K27ac ChIP-seq recovered significantly more STARR-seq peaks than CUT&Tag even when adjusting for genomic coverage (**Supplementary Fig. 6a**) as well as restricting to STARR-seq peaks overlapping open chromatin regions, as profiled by DNase-seq experiments (**Supplementary Fig. 6b**). However, there was no significant difference in the q-value distributions of STARR-seq peaks captured and missed by CUT&Tag and ENCODE, respectively (**Supplementary Fig. 6c**).

Finally, we performed gene ontology enrichment analysis visualizing the top 10 enriched categories with clusterProfiler[39]. Overall, CUT&Tag recovered almost all top ENCODE K562 H3K27ac ChIP-seq ontology terms, including cell adhesion molecule binding, RNA-acting catalytic activity, and cadherin binding, with the exception of the most poorly performing antibodies (**Fig. 6c**). The correspondence of enriched terms indicates that although CUT&Tag may not recover all K562 ChIP-seq peaks, it performs sufficiently well to approximate the K562 regulatory landscape. We further conducted motif analysis with HOMER[40], using all peaks from each sample. Plotting the union of the top 15 enriched transcription factors in each sample revealed that most CUT&Tag samples detected key ENCODE H3K27ac TFBMs, including those for the TFs *Bach1*, *Bach2*, *Elk1*, *Elk4*, *Gata1*, *Gata2*,, *Gata6*, *Jun-AP1*, *Nrf2* and *NF-E2* (**Fig. 6d**), which relate to cell growth[41] and hematological cell fate[42,43]. CUT&Tag also detected TFBMs not captured by ENCODE H3K27ac, such as those for *Elk1*, *Elk4* and *ETS*, which are transcription factors involved in hematopoiesis [44] in line with the K562 lineage (lymphoblast), and this was observed when calling peaks with both SEACR and MACS2 (**Supplementary Fig. 7**). H3K27me3 samples showed more variable and modest TFBM enrichment, which is expected given that the vast majority of transcription factors bind in regions of open chromatin.

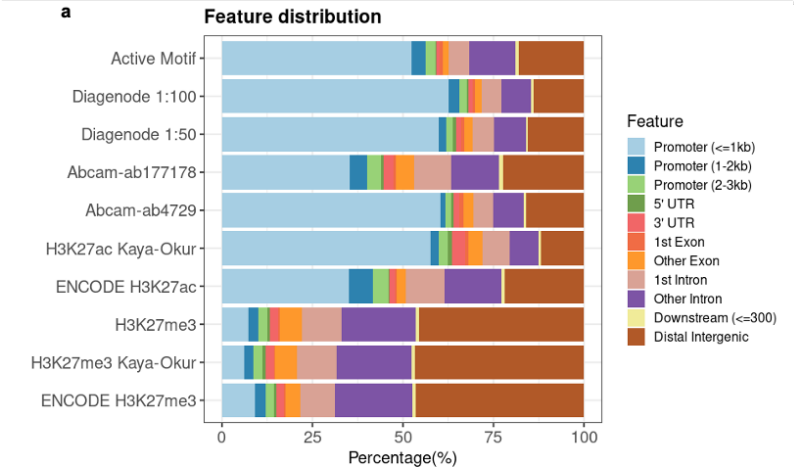
a
Feature distribution
Active Motif
Diagenode 1:100
Diagenode 1:50
Abcam-ab177178
Abcam-ab4729
H3K27ac Kaya-Okur
ENCODE H3K27ac
H3K27me3
H3K27me3 Kaya-Okur
ENCODE H3K27me3
0
25
50
75
100
Percentage(%)
Feature
Promoter (<=1kb)
Promoter (1-2kb)
Promoter (2-3kb)
5' UTR
3' UTR
1st Exon
Other Exon
1st Intron
Other Intron
Downstream (<=300)
Distal Intergenic

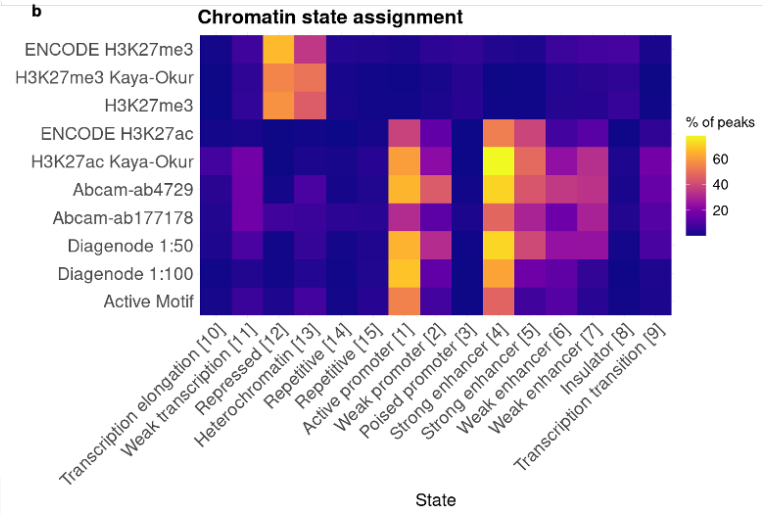
b
Chromatin state assignment
ENCODE H3K27me3
H3K27me3 Kaya-Okur
H3K27me3
ENCODE H3K27ac
H3K27ac Kaya-Okur
Abcam-ab4729
Abcam-ab177178
Diagenode 1:50
Diagenode 1:100
Active Motif
Transcription elongation [10]
Weak transcription [11]
Repressed [12]
Heterochromatin [13]
Repetitive [14]
Repetitive [15]
Active promoter [1]
Weak promoter [2]
Poised promoter [3]
Strong enhancer [4]
Strong enhancer [5]
Weak enhancer [6]
Weak enhancer [7]
Insulator [8]
Transcription transition [9]
State
% of peaks
60
40
20

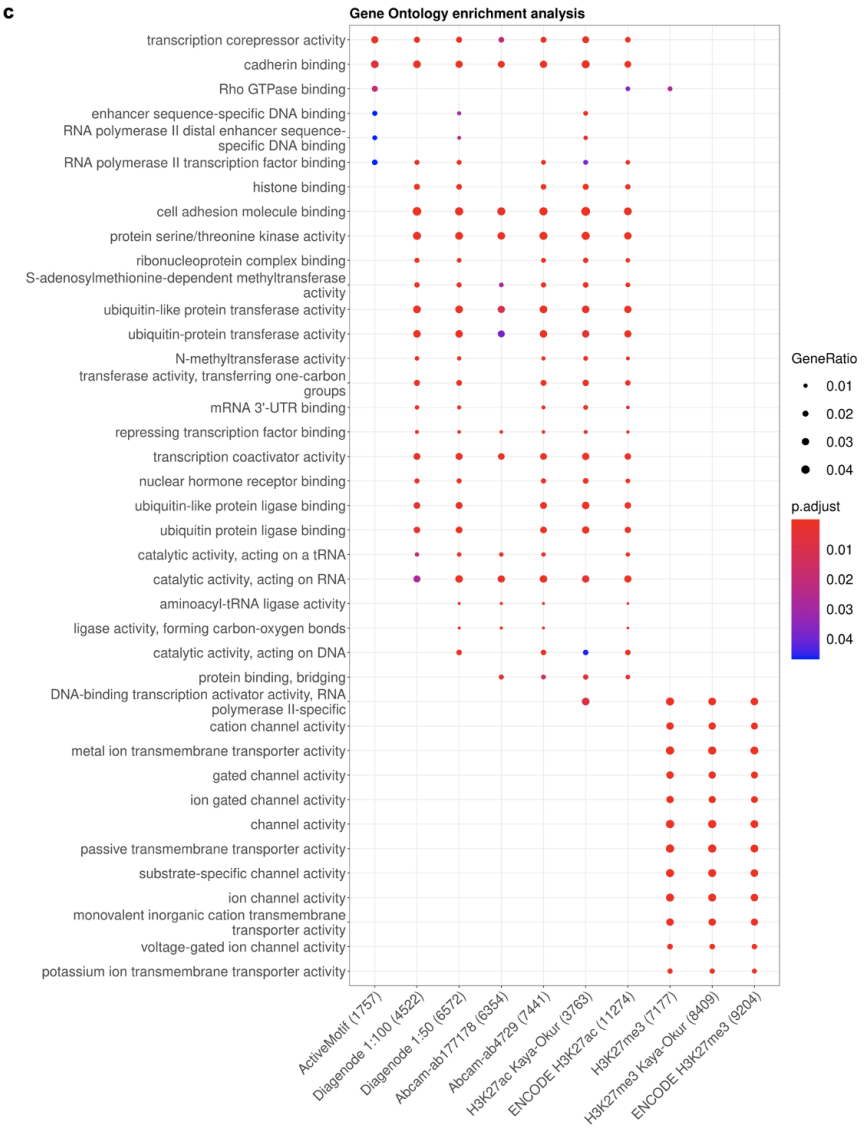
c
Gene Ontology enrichment analysis
transcription corepressor activity
cadherin binding
Rho GTPase binding
enhancer sequence-specific DNA binding
RNA polymerase II distal enhancer sequence-specific DNA binding
RNA polymerase II transcription factor binding
histone binding
cell adhesion molecule binding
protein serine/threonine kinase activity
ribonucleoprotein complex binding
S-adenosylmethionine-dependent methyltransferase activity
ubiquitin-like protein transferase activity
ubiquitin-protein transferase activity
N-methyltransferase activity
transferase activity, transferring one-carbon groups
mRNA 3'-UTR binding
repressing transcription factor binding
transcription coactivator activity
nuclear hormone receptor binding
ubiquitin-like protein ligase binding
ubiquitin protein ligase binding
catalytic activity, acting on a tRNA
catalytic activity, acting on RNA
aminoacyl-tRNA ligase activity
ligase activity, forming carbon-oxygen bonds
catalytic activity, acting on DNA
protein binding, bridging
DNA-binding transcription activator activity, RNA polymerase II-specific
cation channel activity
metal ion transmembrane transporter activity
gated channel activity
ion gated channel activity
channel activity
passive transmembrane transporter activity
substrate-specific channel activity
ion channel activity
monovalent inorganic cation transmembrane transporter activity
voltage-gated ion channel activity
potassium ion transmembrane transporter activity
ActiveMotif (1757)
Diagenode 1:100 (4522)
Diagenode 1:50 (6572)
Abcam-ab177178 (6354)
Abcam-ab4729 (7441)
H3K27ac Kaya-Okur (3763)
ENCODE H3K27ac (11274)
H3K27me3 (7177)
H3K27me3 Kaya-Okur (8409)
ENCODE H3K27me3 (9204)
GeneRatio
0.01
0.02
0.03
0.04
p.adjust
0.01
0.02
0.03
0.04

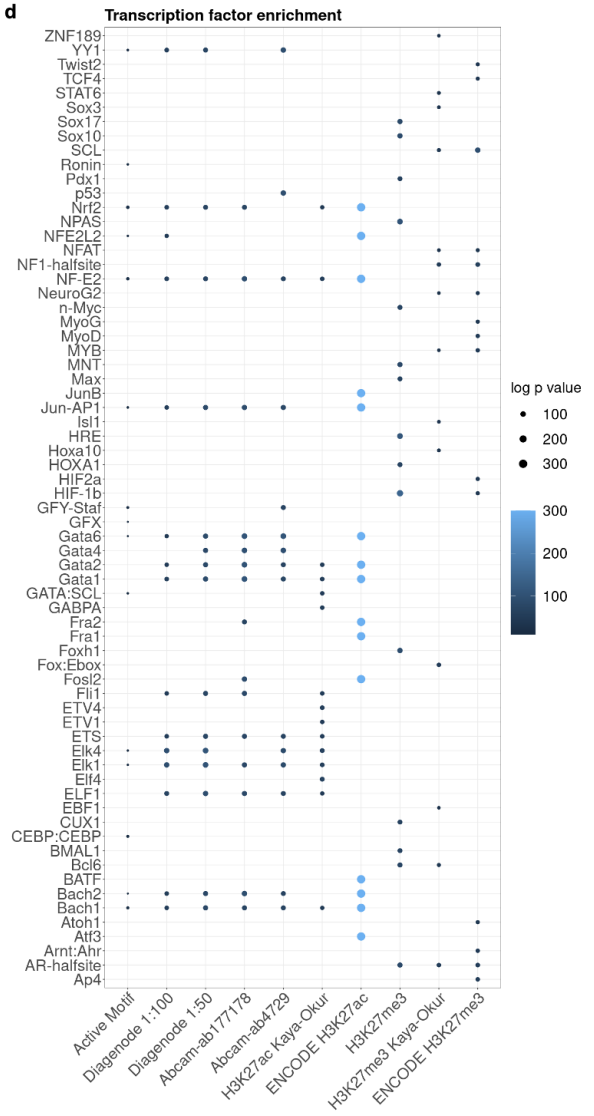
d
Transcription factor enrichment
ZNF189
YY1
Twist2
TCF4
STAT6
Sox3
Sox17
Sox10
SCL
Ronin
Pdx1
p53
Nrf2
NPAS
NFE2L2
NFAT
NF1-halfsite
NF-E2
NeuroG2
n-Myc
MyoG
MyoD
MYB
MNT
Max
JunB
Jun-AP1
Isl1
HRE
Hoxa10
HOXA1
HIF2a
HIF-1b
GFY-Staf
GFX
Gata6
Gata4
Gata2
Gata1
GATA:SCL
GABPA
Fra2
Fra1
Foxh1
Fox:Ebox
Fosl2
Fli1
ETV4
ETV1
ETS
Elk4
Elk1
Elf4
ELF1
EBF1
CUX1
CEBP:CEBP
BMAL1
Bcl6
BATF
Bach2
Bach1
Atoh1
Atf3
Arnt:Ahr
AR-halfsite
Ap4
Active Motif
Diagenode 1:100
Diagenode 1:50
Abcam-ab177178
Abcam-ab4729
H3K27ac Kaya-Okur
ENCODE H3K27ac
H3K27me3
H3K27me3 Kaya-Okur
ENCODE H3K27me3
log p value
100
200
300
300
200
100

Figure 6. Functional analysis of CUT&Tag peaks. a, ChIPseeker assignment of peaks with regulatory elements; **b**, ChromHMM assignment of peaks with chromatin states, showing the relative percentages of total peaks falling into each category (note that peaks can fall into multiple categories simultaneously); **c**, Gene ontology enrichment analysis results of genes assigned to sample peaks ('gene ratio' reflects the proportion of total differentially expressed genes falling into a particular GO term); **d**, Top significantly enriched motifs across all samples.

Discussion

Here we optimized conditions for the execution and analysis of CUT&Tag for H3K27 histone marks, benchmarking its performance against matched ENCODE ChIP-seq reference datasets. We studied H3K27ac in depth, due to its functional co-localization with active promoters and enhancers, relevance for mapping risk variants in complex human disease, and the lack of previous literature optimizing CUT&Tag for acetylation marks. We systematically assessed experimental optimizations including antibody selection, antibody concentration, DNA extraction method, use of enzymatic inhibitors of deacetylases and PCR cycles. We assessed analysis methods exploring the performance of different peak callers SEACR and MACS2, peak calling parameters, and inclusion versus exclusion of duplicates, as a consensus regarding these has been lacking in the field.

On the whole, H3K27ac CUT&Tag successfully recovers many features of ENCODE ChIP-seq and captures the most significant ENCODE peaks. However, across all individual samples, CUT&Tag only recovers up to half of ENCODE peaks. Additionally, CUT&Tag appears to generate distinct peak profiles that favor H3K27ac domains coinciding with open chromatin regions and does not capture less significant ENCODE peaks, which are less enriched in open chromatin. It is uncertain whether this is a result of CUT&Tag failing to capture some finer but nevertheless relevant ChIP-seq peaks, or an indicator that ENCODE ChIP-seq may detect less relevant H3K27ac domains that have lower incidence of open chromatin, an important feature of active regulatory elements. Thus, although ENCODE ChIP-seq is often used as a standard reference dataset, it is unclear exactly how well ENCODE data reflects the ground truth. ChIP-seq peaks missed by CUT&Tag could potentially represent noise or false signal detected by ChIP-seq due to chromatin shearing and sonication, as well as fixation and cross-linking resulting in heterochromatin bias[11,12]. Investigation into new methods of chromatin profiling would significantly benefit from inclusion of orthogonal approaches to mapping chromatin modifications and regulatory elements. We used K562 STARR-seq data[30] to estimate the capture of enhancer regions by both CUT&Tag and ENCODE, and found that ENCODE recovers a greater number of putative enhancers, and does so with higher efficiency. However, since STARR-seq identifies regulatory elements independently of chromatin context, such an analysis is ideally restricted to cell-specific active regulatory elements (by using ENCODE DNase-seq data). Benchmarking was also attempted with massively parallel reporter assay (MPRA) data[45], but the most significant regulatory assay quantitative trait loci (raQTLs) did not appear to be enriched in

enhancer and promoter elements, and their coordinates could not be used as proxies for their genomic locations. Thus, currently available MPRA data cannot serve this benchmarking purpose. Going forward, it would be helpful to determine whether H3K27ac ChIP-seq peaks that are not captured can be functionally validated.

The capabilities of CUT&Tag likely also vary depending on histone mark, given the better performance of H3K27me3. It should be noted that the H3K27me3 antibody used is monoclonal, whereas the H3K27ac antibodies used are all polyclonal except for monoclonal Abcam-ab177178, which did not perform as well as polyclonal Abcam-4729. Because our best performing antibody in H3K27ac CUT&Tag is the same as that used for ENCODE ChIP-seq (Abcam 4729), this could have contributed to its favorable result in ENCODE overlap and comparisons. Analysis of both current and comparison data showed that CUT&Tag achieves a maximum of ~50% ENCODE coverage for the H3K27ac mark, and capture was modestly improved to ~60% when using an aggregate sample. CUT&Tag appears to perform better for methyl marks than for H3K27ac, and in the literature, the superiority of CUT&Tag over ChIP-seq was demonstrated on methyl marks[15]. However, it should be noted that our assessment of ENCODE capture by HCT116 CUT&Tag suggests that this might not always be the case. We found that peak calling parameters can greatly influence quality measures, such as FRiPs, and should be adjusted depending on histone modification. Nevertheless, it is uncertain why H3K27ac did not yield itself as well to CUT&Tag in K562 cells. A possibility is that acetylation marks may be more dynamic, e.g. in response to environmental triggers, while methylation marks tend to be more stable [46]. With limited cell numbers, a dynamically modulated histone mark may appear to display more noise. It would be interesting to see whether the same issues are encountered when profiling other acetyl marks, which has not yet been systematically addressed.

Presence of high duplication rates could be a result of overamplification during library preparation or over-sequencing. In either case duplicates can be removed without compromising data quality. An advantage of high sequencing depths is sample saturation, meaning that the vast majority of unique fragments present in each sample was recovered; however, one intended advantage of CUT&Tag relative to methods such as ChIP-seq is the ability to recover comparable or superior levels of information at lower sequencing depths. Fractions of reads in ENCODE H3K27ac peaks were approximately equal with and without duplicates, suggesting that they are evenly distributed. Consequently, duplicates made little to no difference when calling peaks with SEACR, since genuine H3K27ac reads contributed to peaks that would in any case be called without duplicates, and reads outside genuine peaks did not meet the peak calling threshold. However, duplicates resulted in the detection of a significant number of spurious peaks with MACS2, many of which fell into heterochromatic regions, which should not be marked by H3K27ac[7]. Therefore, there is marginal gain in recall (ENCODE capture) with retention of duplicates at the expense of precision (detection of spurious peaks). Using fewer PCR cycles during library preparation appears to modestly reduce duplication rates without significantly influencing ENCODE capture.

Peak calling settings can have a significant effect on the perceived outcomes of chromatin profiling experiments. In this study, multiple peak calling parameters were tested and selected on the basis of precision and recall against matched ENCODE ChIP-seq profiles. MACS2 and SEACR performed similarly, in spite of the marked differences in peak definition between the two peak callers. However, achieving optimal performance with MACS2 required significantly more optimization. Which approach is correct is debatable because there is no strict definition as to what qualifies as a 'peak', but one concern is that peak calling with SEACR might make it difficult to detect subtle changes in histone marks, due to its tendency to call wider peaks and combine multiple potentially distinct H3K27ac domains into single peaks. We did not find a significant difference in promoter-enhancer merging by the two peak callers, although SEACR appears to attain higher capture of putative enhancers with fewer called sample peaks outside promoter regions. With regards to differences in precision, MACS2 was optimized specifically for ChIP-seq. ChIP-seq samples are normally sequenced to much higher read depths and tend to possess higher levels of background, which is why MACS2 is designed to identify signal in data with high levels of noise[29,47]. In principle, CUT&Tag and CUT&RUN have reduced background as the only DNA fragments that are released are those bound by the protein of interest[15,48]. CUT&RUN is likely to be superior for mapping transcription factor binding, as CUT&Tag employs elevated salt conditions for pA-Tn5 binding to prevent tagmentation of accessible DNA. This in turn can strip away transcription factor-DNA interactions, while histone modifications stay intact [19]. For a peak caller like MACS2, any off-target reads in samples with low background might be perceived as legitimate peaks, and this may explain why the inclusion of duplicates gave rise to spurious peaks. Notably, our analyses did not confirm higher signal-to-noise ratio for H3K27ac CUT&Tag compared to ENCODE ChIP-seq profiles. Rather we found H3K27ac CUT&Tag to display equal or higher noise, in contrast to what is seen for H3K27me3 and other methyl marks in our analyses and previously reported by others. When restricting the interrogated regions to ChIP-seq and CUT&Tag-overlapping ranges to address the confounding effects of differential peak calling, H3K27ac CUT&Tag produced very similar FRiP scores to ChIP-seq, whereas H3K27me3 CUT&Tag showed significantly improved performance. Whether this represents a general challenge for CUT&Tag of histone acetylation marks remains to be explored further. In the future, more specific peak calling methods designed for CUT&Tag data, such as the recently reported method GoPeaks[49], are likely to improve performance of CUT&Tag profiling and should be included in future comparisons for benchmarking analysis.

The lack of established metrics to standardize performance makes it challenging to compare peak callers. Precision cutoffs are arbitrary and there is opportunity to significantly increase recall at the expense of precision even within a predetermined boundary. Going forward, it might be worth characterizing the CUT&Tag peaks that could be obtained without strict limits on precision to determine whether they could be legitimate peaks that are not captured by H3K27ac ChIP-seq. For example, it has been suggested that the relatively low correlation between CUT&RUN and ChIP-seq may be due to CUT&RUN's superior ability to map repetitive, difficult regions that are typically not covered by ChIP-seq[50]. There is some indication of this as CUT&Tag and CUT&RUN samples processed with SEACR were far more enriched in weak enhancers and weakly transcribed regions than ENCODE ChIP-seq, but MACS2

ChromHMM profiles differed minimally from ENCODE and this analysis indicated that this effect is more likely a result of peak caller selection rather than being intrinsic to CUT&Tag. One limitation associated with the use of ChromHMM annotations is that chromatin states are inferred on the basis of broad ENCODE ChIP-seq peaks, which introduces some circularity into overlap analysis with ENCODE H3K27ac peaks. Thus, states which occur in CUT&Tag but not in ENCODE H3K27ac are those that should in principle not contain the H3K27ac mark. However, these annotations draw upon combinations of histone marks[51], and still give some indication as to where a particular modification might or might not be expected to occur.

The improved sensitivity of CUT&Tag compared to ChIP-seq is due to the use of pA-Tn5 to streamline library preparation through direct insertion of PCR sequencing adapters via *in situ* tagmentation. However, its sensitivity is inherently limited by PCR, since pA-Tn5 inserts its adapters in random orientations such that approximately half of the targets do not have adapters in the correct orientation to amplify. In addition, PCR library preparation is highly sensitive to size variations of amplicons. When two adjacent transposition events occur too far apart, they will not amplify efficiently during PCR or sequencing cluster generation. However, when they are too close, they will exponentially bias library coverage due to increased PCR amplification and clustering efficiency of shorter fragments. One recent approach that may help overcome some of these issues is linear amplification by Targeted Insertion of Promoters (TIP-seq[16,34]). In TIP-seq, a pA-Tn5 fusion protein is used to insert a T7 RNA polymerase promoter near sites occupied by transcription factor or histone mark of interest. The promoter facilitates linear amplification of DNA in its vicinity using a T7 polymerase to create 1,000-fold RNA copies of insertion sites. The distance between two transposition sites does not bias library preparation since only one T7 promoter is needed to amplify the site of interest. Linear amplification generates greater fidelity and uniformity, as mistakes made during amplification do not themselves become templates to exponentially propagate errors – this results in higher mappability of single cell sequencing reads[52]. TIP-seq was shown to generate single cell libraries with higher read coverage, greater library complexity, and lower background, with a higher proportion of unique, non-duplicated reads per cell compared to CUT&Tag[34]. Comprehensive optimization and benchmarking of this novel technique will be essential moving forward.

Conclusions

CUT&Tag has been reported as a more streamlined, cost-effective approach to chromatin profiling, but despite a definite correspondence with ENCODE ChIP-seq, CUT&Tag consistently achieves an ENCODE coverage ceiling of approximately 50%. Furthermore, the performance of this method appears to vary by histone mark. Additional analysis will be required to better characterize the inconsistencies between CUT&Tag and ENCODE ChIP-seq. Optimizing experimental parameters, our analysis established Abcam-ab4729 as the top-performing antibody for H3K27ac and demonstrated that the use of an HDACi does not improve H3K27ac CUT&Tag performance. Duplicates can and should be discarded, particularly beyond a threshold at which they start to contribute more off-target than on-target information. The

optimal choice of peak caller is debatable, but SEACR attains the best possible performance with very little optimization and is more impervious to identification of spurious peaks. There is also some evidence that it calls peaks with greater consistency than MACS2, even on the basis of poorer-quality reads and lower sequencing depths. We observe that fewer PCR cycles reduced duplication rates, but at the expense of ENCODE recovery and capture. We provide benchmarking pipeline EpiCompare[18] to aid researchers in optimally analyzing and interpreting their CUT&Tag datasets. We hope that our systematic optimizations of CUT&Tag will help to facilitate its more widespread adaptation in the field and expedite its application in understanding the epigenetic causes and consequences of complex diseases.

Methods

Biological materials

Human K562 cells were obtained from ATCC (Manassas, VA, Catalog #CCL-243) and cultured according to the supplier's protocol. Mycoplasma was tested to be negative for all cellular input reported using Mycoplasma Detection Kit (Jena Bioscience PP-401) following manufacturer's instructions. The following antibodies were used: Guinea Pig anti-Rabbit IgG (Heavy & Light Chain) Preabsorbed antibody (Antibodies-Online ABIN101961), H3K27me3 (Cell Signaling Technology, 9733, Lot 14), H3K27ac (Abcam ab177178, Lot GR3202987-5), H3K27ac (Active Motif 39133, Lot 16119013), H3K27ac (Abcam ab4729, Lot G3374555-1), H3K72ac (Diagenode C15410196, Lot A1723-0041D). The following histone deacetylase inhibitors were used: Sodium butyrate (Merck B5887-250MG; used at 5 mM in CUT&Tag solutions with HDACi treatment), Trichostatin A (Enzo Life Sciences BML-GR309-0001; used at 1 μM in CUT&Tag solutions with HDACi treatment). The following commercial loaded protein A-Tn5 transposase fusion protein (pA-Tn5) were used at recommended dilutions by the manufacturer: CUTANA™ pAG-Tn5 (Epicypher 15-1017; Lot 20142001-C1), or pA-Tn5 Transposase - loaded (Diagenode C01070001; Lot 1/b/b).

CUT&Tag nuclei processing

Bench top CUT&Tag was performed as previously described (https://www.protocols.io/view/bench-top-cut-amp-tag-bcuhiwt6)[15]. Exponentially growing K562 cells were harvested, counted and centrifuged for 3 min at 600*g* at room temperature (RT). 500,000 cells per condition were washed twice in 1 mL Wash Buffer (20 mM HEPES-KOH pH 7.5, 150 mM NaCl, 0.5 mM Spermidine, 1x Protease inhibitor cocktail; Roche 11836170001). Nuclei were extracted by incubating cells for 10 minutes on ice in 200 μL/sample of cold Nuclei Extraction buffer (NE buffer: 20 mM HEPES-KOH pH 7.9, 10 mM KCl, 0.1% Triton X-100, 20% Glycerol, 0.5 mM Spermidine, 1x Protease Inhibitor cocktail). Following incubation in NE buffer, nuclei were centrifuged for 3 min at 600g at RT, then resuspended in 100 μL cold NE buffer. Concanavalin A coated magnetic beads (Bangs Laboratories BP531) were prepared as

previously described [48]and 11 µL of activated beads were added per sample into PCR strip tubes and incubated at RT with gentle rocking for 10 min. Beads were placed on a magnetic rack and unbound supernatant was discarded. Bead bound nuclei were resuspended in 50 µL Dig-wash Buffer (20 mM HEPES pH 7.5, 150 mM NaCl, 0.5 mM Spermidine, 1× Protease inhibitor cocktail, 0.05% Digitonin) with 2 mM EDTA and 0.1% BSA. 1:50/1:100/1:200 dilution of primary antibody was added, followed by a gentle vortex and brief spin. Primary antibody incubation was conducted on a rotating platform overnight at 4°C. Primary antibody solution was removed by placing the PCR tube on a magnetic rack, allowing the solution to fully clear, then removing the supernatant. Next, the appropriate secondary antibody, Guinea Pig anti-Rabbit IgG antibody for a rabbit primary antibody, was added at 1:100 in Dig-Wash buffer and incubated at RT with rotation for 30-60 min. Nuclei were washed twice in 200 µL Dig-Wash buffer using a magnetic rack to remove unbound antibodies in supernatant. Nuclei were resuspended in 50 µL Dig-med Buffer (20 mM HEPES pH 7.5, 300 mM NaCl, 0.5 mM Spermidine, 1× Protease inhibitor cocktail, 0.05% Digitonin), then 1:20 CUTANA™ pAG-Tn5 (Epicypher 15-1017), or 1:250 pA-Tn5 Transposase -loaded (Diagenode C01070001) was added, gently mixed and spun down. pA-Tn5 binding occurred at RT for 1 hour on a rotating platform. To remove unbound pA-Tn5, nuclei were washed twice in 200 µL Dig-med Buffer. Nuclei were then resuspended in 50 µL Tagmentation buffer (10 mM $MgCl_2$ in Dig-med Buffer) and incubated at 37°C for 1 hour to activate transposase enzymatic activity. Next, either column or sodium dodecyl sulfate (SDS) based DNA extraction was conducted.

Column DNA extraction

To stop tagmentation and solubilize DNA fragments, the following were added to each 50 µL sample: 1.68 µL 0.5M ethylenediaminetetraacetic acid (EDTA), 0.5 µL 10% SDS, 0.44 µL 10 mg/mL Proteinase K. The samples were briefly mixed and vortexed at full speed for ~2 seconds, then incubated at 55°C for 1 hour to digest the DNA. After a quick spin, tubes were placed on a magnetic rack and solution was allowed to clear. Supernatant was carefully transferred to a new 1.5 mL microcentrifuge tube, then sample processing protocol of ChIP DNA Clean & Concentrator (Zymo Research D5205) was executed, eluting with 21 µL Elution Buffer.

SDS-based DNA extraction

Following tagmentation at 37°C for 1 hour, PCR tubes were placed on a magnetic rack and solution was allowed to clear. Supernatant was removed carefully, then beads were resuspended thoroughly in 50 µL [tris(hydroxymethyl)methylamino]propanesulfonic acid (TAPS) Buffer (10 mM TAPS pH 8.5, 0.2 mM EDTA) at RT. Tubes were returned to a magnetic rack and supernatant was removed. 5 µL SDS Release Buffer (10 mM TAPS pH 8.5, 0.1% SDS) was added at RT to each sample and tubes were vortexed at full speed for ~10 seconds. After a quick spin, ensuring no beads are stuck to the side of the tubes, samples were incubated at 58°C for 1 hour. Next, 15 µL SDS Quench Buffer (0.67% Triton-X 100 in Molecular grade H_2O) was added at RT and vortexed at maximum speed to neutralize the SDS prior to PCR library amplification.

CUT&Tag PCR-based library amplification

For library amplification in PCR tube format, 21 µL DNA was combined with 2 µL of universal i5 and uniquely barcoded i7 primer[53] where a different barcode was used for each sample that was intended to be pooled together. 25 µL NEBNext HiFi 2× PCR Master mix was added, then the sample was gently mixed through and spun down. The sample was placed in a Thermocycler with heated lid following these conditions: 72°C for 5 min (gap filling); 98°C for 30 s; 11-15 cycles of 98°C for 10 s and 63°C for 30 s; final extension at 72°C for 1 min; and hold at 4°C. Following PCR, bead cleanup was conducted by addition of 1.1x Ampure XP beads (Beckman Coulter). Library and beads were mixed thoroughly, then spun down and incubated at RT for 10-15 min. Beads were gently washed twice with freshly prepared 80% ethanol using a magnetic rack, then the library was eluted with 20-30 µL 10 mM Tris-HCl pH 8.0 at RT.

Sequencing

Final library size distributions were assessed by Agilent 2100 Bioanalyser and Agilent 4200 TapeStation for quality control before sequencing. Libraries were pooled to achieve equal representation of the desired final library size range (equimolar pooling based on Bioanalyser/TapeSation signal in the 150bp to 800bp range). Paired-end Illumina sequencing using the HiSeq 4000 PE75 strategy was conducted on barcoded libraries at Imperial Biomedical Research Centre (BRC) Genomics Facility following manufacturer's protocols.

qPCR

Quantitative real-time PCR (qPCR) was performed following manufacturer's instructions in triplicate technical and triplicate biological replicates (https://www.thermofisher.com/order/catalog/product/4309155#/4309155). Positive and negative control primers were designed based on ENCODE peaks ranked highest to lowest, respectively.

Gene	Control type	Primer sequence (5'→3')
ARHGAP22	Positive	Fw: GCTGAGAAGGAAGGGCTTAAT Rv: GCTAGTCGGGATGATTTACAGG
COX4I2	Positive	Fw: GGATACCTCCAAGGCTTCATAC Rv: GTAGTCACAGAACTAGGGTTGG
MTHFR	Positive	Fw: GGGTGGAACATCTCGAACTATC Rv: GAACGAAGCCAGAGGAAACA
ZMYND8	Positive	Fw: GGATCTACAAACTTCCCTTCCC

		Rv: GAAGGCATCGCAGGCTAATA
KLHL11	Negative	Fw: GACAAGCAGTGGCTCTACAA Rv: CAGTATCGGAAAGAAGCCTACC
SIGIRR	Negative	Fw: CCAAGCTCAGACCTCAAAGT Rv: TTCTTGCTGTGCTCGTATCC

Table 1. qPCR primer sequences. Control primer sequences based on ENCODE peaks.

Levels of H3K27ac CUT&Tag binding signal was determined by qPCR amplification carried out with the QuantStudio™ 5 Real-Time PCR System (ThermoFisher A34322) using the Standard Curve experiment type and SYBR Green Master Mix (ThermoFisher 4309155). Each qPCR condition was conducted with triplicate repeats and the data was analyzed using the 2^-ΔΔ*CT* method where each CUT&Tag sample was normalized to qPCR levels of K562 genomic DNA (gDNA) run in parallel. qPCR results were calculated using the equation:

$$2^{-(CT\ sample\ -\ CT\ gDNA)}$$

Data processing

The full dataset, i.e. paired-end reads were used for the analysis. Sequencing data was processed according to the CUT&Tag Data Processing and Analysis Tutorial (https://yezhengstat.github.io/CUTTag_tutorial), with some alterations. Raw sequencing reads were trimmed using TrimGalore (version 0.6.6; https://github.com/FelixKrueger/TrimGalore) to remove adapters and low-quality reads. The trimmed fastq files were aligned to hg19 using bowtie (version 2.2.9; [54]) with the following parameters: *--local --very-sensitive --no-mixed --no-discordant --phred33 -I 10 -X 700*. PCR duplicates were removed using Picard (version 2.6.0; http://broadinstitute.github.io/picard/), and bam and fragment bed files from original and deduplicated alignments were generated using samtools (version 1.3.1;[55]) and bedtools (version 2.25.0;[56]), selecting for fragment lengths under 1000 bp. Peaks were called using MACS2 (Model-based Analysis of ChIP-seq; version 2.1.4) [47] and SEACR (Sparse Enrichment Analysis for CUT&RUN; version 1.3)[26]. MACS2 peaks were called as follows: *macs2 callpeak -t input_bam -n sample_name -f BAMPE -g hs -q 1e-5 --keep-dup all –nolambda --nomodel --outdir out_dir*. SEACR peaks were called on the basis of fragment bedgraph files generated with bedtools genomecov. SEACR peaks were called as follows: *SEACR_1.3.sh input_bedgraph 0.01 non stringent out_name*. In both cases other combinations of peak calling settings were also tested (see **Results**). To test peak calling performance with control data, published IgG CUT&Tag replicate libraries (SRR8754611 and SRR8754612; study accession PRJNA512492)[15] were downloaded in fastq format from the European Nucleotide Archive[57] (https://www.ebi.ac.uk/ena/browser/home), pooled together, and processed as described to produce bam and bedgraph files as inputs for MACS2 and SEACR; otherwise, peaks were called using previously selected parameters. Motifs were identified from complete peak sets using

HOMER (Hypergeometric Optimization of Motif EnRichment; version 4.10;[40]) as follows: *findMotifsGenome.pl input_bed hg19 out_dir -size 1000*. Downsampled bam files were generated by random sampling of original bam files as follows, where {x} represents the seed value and {y} the fraction of total read pairs to be sampled: *samtools view -bs {x}.{y} input_bam > downsampled_bam*.

To more closely approximate the replicated peaks strategy employed by ENCODE, pooled peaks were called with SEACR (at a cutoff threshold of 0.1) after merging bam files across all CUT&Tag H3K27ac samples generated in this study (5 samples total). This procedure was repeated using both our internal samples and previously published samples from (7 samples total). This procedure was carried out by running the *pooled_peaks* function in the R package PeakyFinders (https://github.com/neurogenomics/PeakyFinders). *EpiCompare* was then run on each set of pooled peak files separately to generate precision-recall curves.

Sample comparisons

Published CUT&Tag[15] and CUT&RUN[20] samples were obtained as fastq files from the European Nucleotide Archive (study accessions PRJNA512492 and PRJNA522731, respectively) and processed as described above. Peak-level correlations were obtained with the DiffBind package (version 3.0.15;[31]). Genome-wide sample correlations were carried out using bedtools multicov against hg19 split into 500bp bins. Read counts were then quantile-normalized and rounded to the nearest integer, and heatmaps plotted in R[58] based on sample-by-sample Pearson correlations of the processed counts. Fingerprint plots were generated from sample and ENCODE bam files using deepTools (version 3.5.1;[59]) plotFingerprint, setting genome-wide bin sizes of 1000bp. Heatmaps were plotted using deeptools computeMatrix and plotHeatmap to visualise read enrichment around hg19 transcription start sites (obtained from NCBI RefSeq) and peak summits. For these ends, ENCODE H3K27ac and H3K27me3 samples (ENCSR000AKP and ENCSR000EWB, respectively) were run through the ENCODE histone ChIP-seq pipeline (https://github.com/ENCODE-DCC/chip-seq-pipeline2), with replicates downsampled to 1 million reads per sample and pooled together. Likewise, to plot heatmaps, paired-end CUT&Tag sample bam files were downsampled to 2 million fragments (4 million reads) and only the first of the read mates mapped to yield a total of 2 million mapped reads. As a weighted average of precision and recall, F1-scores were calculated as follows, where *tp*, *fp*, and *fn* represent the numbers of true positive, false positive, and false negative CUT&Tag peaks, respectively:

$$F1 = \frac{tp}{tp + 1/2(fp + fn)}$$

Downstream data analysis

Downstream analysis, including quality control, ENCODE benchmarking, and regulatory element annotation, were performed in R[58]. Peak overlaps were determined with the GenomicRanges package (version 1.38.0;[33]). All peaks overlapping with hg19 blacklisted regions (ENCODE ID: ENCFF000KJP) were removed prior to downstream analysis. Peaks falling into mitochondrial or

other non-standard chromosomes were also excluded using BRGenomics (version 1.1.3; https://mdeber.github.io). FRiP scores were calculated using the chromVAR package (version 1.8.0;[60]). ATAC-seq libraries (ENCODE IDs: ENCLB918NXF and ENCLB758GEG) used for FRiP analysis were processed with the nf-core ATAC-seq pipeline [61]. To calculate FRiP scores in overlapping ENCODE and CUT&Tag peak regions, CUT&Tag peak ranges intersecting with ENCODE H3K27ac replicated narrow peaks (ENCFF044JNJ) and H3K27me3 replicated broad peaks (ENCFF000BXB) were obtained using the bedtools intersect tool; the same peak files were used for ENCODE capture calculations. This was performed for each sample-ENCODE pair. For the calculation, pooled reads from ENCODE H3K27ac ChIP-seq replicates ENCFF384ZZM and ENCFF070PWH, and H3K27me3 ChIP-seq replicates ENCFF000BXA and ENCFF000BXC, were used. To determine precision and recall of ENCODE peak capture in the HCT116 cell line, H3K27me3 narrow peaks (ENCFF255ARD) and published H3K27me3 CUT&Tag data (study accession: PRJNA779107; sample accession: SRR16963158) were used[34]. Regulatory element annotation was performed using ChIPseeker (version 1.22.1;[62]), after annotating peaks with genes using the TxDb.Hsapiens.UCSC.hg19.knownGene database (version 3.2.2;[63]). To identify promoter-overlapping peaks, this database was also used as input to the ChIPseeker getPromoters function to obtain genomic ranges 1.5Kb upstream and downstream of known promoters. ChromHMM annotations assigned with genomation (version 1.18.0;[37]). To test for enhancer enrichment, STARR-seq peak files (ENCFF717VJK and ENCFF394DBM) were processed to keep only replicated peaks, and lifted over to hg19 using the rtracklayer liftOver function [64]. To obtain putative cell-specific enhancers, STARR-seq peak ranges were filtered to keep those overlapping with K562 DNase-seq peaks (ENCODE ID: ENCFF722NSO). Functional enrichment analysis was carried out with clusterProfiler (version 3.13.4;[65]), using the "enrichGO" function. Results from motif analysis were processed with marge (version 0.0.4.9999, https://github.com/robertamezquita/marge). For visualization with the Integrative Genomics Viewer (IGV; v2.9.4) [27], sample bedgraphs were converted to bigwig files using the UCSC Genome Browser bedGraphToBigWig binary. Single ENCODE replicate bam files (H3K27ac: ENCFF384ZZM; H3K27me3: ENCFF000BXA) were converted to bedgraphs with bedtools genomecov[56], and similarly converted to bigwig format.

Data and code availability

Fastq and peak files have been deposited in the Gene Expression Omnibus (GEO) under accession GSE199611. Code used in this study is available in the dedicated GitHub repository: https://github.com/neurogenomics/CUTnTag-benchmarking-analysis

Bigwig, bedgraph and peak files can be found at: https://webserver-schilder-ukdri.dsi.ic.ac.uk/cutntag_benchmarking/

Sample bigwig tracks can be found at: http://genome-euro.ucsc.edu/s/bschilder/cutntag_benchmarking

Generalized code for performing comparisons between genome-wide histone modification profiles has been made available as an R package via Github at https://github.com/neurogenomics/EpiCompare.

Authors' contributions

All authors conceived the study. DH performed all laboratory experiments. LA performed computational analyses with guidance and support of BMS. SJM and NGS acquired funding and supervised the study. AN guided study directions and interpretations. All authors wrote, read and approved the manuscript.

Funding

This work was funded by an Alzheimer's Association grant [grant number ADSF-21-829660-C] to SJM and a UKRI Future Leaders Fellowship [grant number MR/T04327X/1] awarded to NGS. SJM and AN are funded by the Edmond and Lily Safra Early Career Fellowship Program. SJM, NGS and AN are funded by the UK Dementia Research Institute, which receives its funding from UK DRI Ltd, funded by the UK Medical Research Council, Alzheimer's Society and Alzheimer's Research UK.

Acknowledgements

We thank the UK DRI Neurogenomics Laboratory (https://www.neurogenomics.co.uk), in particular Alan E Murphy, for feedback, troubleshooting, and guidance in experimental design and analysis. We thank Katiuska Pulgar Prieto for help with K562 mycoplasma testing.

Ethics declarations

Competing interests

The authors declare no competing interests.

References

1. Zhang, F. & Lupski, J. R. Non-coding genetic variants in human disease. *Hum. Mol. Genet.* **24**, R102–10 (2015).
2. Novikova, G. *et al.* Integration of Alzheimer's disease genetics and myeloid genomics identifies disease risk regulatory elements and genes. *Nat. Commun.* **12**, 1610 (2021).
3. Watanabe, K. *et al.* A global overview of pleiotropy and genetic architecture in complex traits. *Nat. Genet.* **51**, 1339–1348 (2019).
4. Fox, S. *et al.* Hyperacetylated chromatin domains mark cell type-specific genes and suggest distinct modes of enhancer function. *Nat. Commun.* **11**, 4544 (2020).
5. Nott, A. *et al.* Brain cell type–specific enhancer–promoter interactome maps and disease-risk association. *Science* **366**, 1134–1139 (2019).
6. Hannon, E., Marzi, S. J., Schalkwyk, L. S. & Mill, J. Genetic risk variants for brain disorders are enriched in cortical H3K27ac domains. *Mol. Brain* **12**, 7 (2019).
7. Creyghton, M. P. *et al.* Histone H3K27ac separates active from poised enhancers and predicts developmental state. *Proc. Natl. Acad. Sci. U. S. A.* **107**, 21931–21936 (2010).
8. Marzi, S. J. *et al.* A histone acetylome-wide association study of Alzheimer's disease identifies disease-associated H3K27ac differences in the entorhinal cortex. *Nat. Neurosci.* **21**, 1618–1627 (2018).
9. Nativio, R. *et al.* An integrated multi-omics approach identifies epigenetic alterations associated with Alzheimer's disease. *Nat. Genet.* **52**, 1024–1035 (2020).
10. Rodríguez-Ubreva, J. & Ballestar, E. Chromatin Immunoprecipitation. in *Functional Analysis of DNA and Chromatin* (eds. Stockert, J. C., Espada, J. & Blázquez-Castro, A.) 309–318 (Humana Press, 2014).

11. Teytelman, L., Thurtle, D. M., Rine, J. & van Oudenaarden, A. Highly expressed loci are vulnerable to misleading ChIP localization of multiple unrelated proteins. *Proc. Natl. Acad. Sci. U. S. A.* **110**, 18602–18607 (2013).
12. Baranello, L., Kouzine, F., Sanford, S. & Levens, D. ChIP bias as a function of cross-linking time. *Chromosome Res.* **24**, 175–181 (2016).
13. Kaya-Okur, H. S., Janssens, D. H., Henikoff, J. G., Ahmad, K. & Henikoff, S. Efficient low-cost chromatin profiling with CUT&Tag. *Nat. Protoc.* **15**, 3264–3283 (2020).
14. Landt, S. G. *et al.* ChIP-seq guidelines and practices of the ENCODE and modENCODE consortia. *Genome Res.* **22**, 1813–1831 (2012).
15. Kaya-Okur, H. S. *et al.* CUT&Tag for efficient epigenomic profiling of small samples and single cells. *Nat. Commun.* **10**, 1930 (2019).
16. Zhu, C. *et al.* Joint profiling of histone modifications and transcriptome in single cells from mouse brain. *Nat. Methods* **18**, 283–292 (2021).
17. Bartosovic, M., Kabbe, M. & Castelo-Branco, G. Single-cell CUT&Tag profiles histone modifications and transcription factors in complex tissues. *Nat. Biotechnol.* **39**, 825–835 (2021).
18. Sera Choi, Brian M. Schilder, Alan Murphy, Nathan G. Skene. *EpiCompare: Comparison, Benchmarking & QC of Epigenetic Datasets*. (2022). doi:doi:10.18129/B9.bioc.EpiCompare.
19. Henikoff, S., Henikoff, J. G., Kaya-Okur, H. S. & Ahmad, K. Efficient chromatin accessibility mapping in situ by nucleosome-tethered tagmentation. *Elife* **9**, (2020).
20. Meers, M. P., Bryson, T. D., Henikoff, J. G. & Henikoff, S. Improved CUT&RUN chromatin profiling tools. *Elife* **8**, (2019).
21. Woodcock, C. L., Skoultchi, A. I. & Fan, Y. Role of linker histone in chromatin structure and

function: H1 stoichiometry and nucleosome repeat length. *Chromosome Res.* **14**, 17–25 (2006).

22. Luger, K., Dechassa, M. L. & Tremethick, D. J. New insights into nucleosome and chromatin structure: an ordered state or a disordered affair? *Nat. Rev. Mol. Cell Biol.* **13**, 436–447 (2012).
23. Yan, F., Powell, D. R., Curtis, D. J. & Wong, N. C. From reads to insight: a hitchhiker's guide to ATAC-seq data analysis. *Genome Biol.* **21**, 22 (2020).
24. Krehenwinkel, H. *et al.* Estimating and mitigating amplification bias in qualitative and quantitative arthropod metabarcoding. *Sci. Rep.* **7**, 17668 (2017).
25. Zhang, Y. *et al.* Model-based analysis of ChIP-Seq (MACS). *Genome Biol.* **9**, R137 (2008).
26. Meers, M. P., Tenenbaum, D. & Henikoff, S. Peak calling by Sparse Enrichment Analysis for CUT&RUN chromatin profiling. *Epigenetics Chromatin* **12**, 42 (2019).
27. Robinson, J. T. *et al.* Integrative genomics viewer. *Nat. Biotechnol.* **29**, 24–26 (2011).
28. Wang, M. & Zhang, Y. Tn5 transposase-based epigenomic profiling methods are prone to open chromatin bias. *bioRxiv* 2021.07.09.451758 (2021) doi:10.1101/2021.07.09.451758.
29. Feng, J., Liu, T., Qin, B., Zhang, Y. & Liu, X. S. Identifying ChIP-seq enrichment using MACS. *Nat. Protoc.* **7**, 1728–1740 (2012).
30. Arnold, C. D. *et al.* Genome-wide quantitative enhancer activity maps identified by STARR-seq. *Science* **339**, 1074–1077 (2013).
31. Ross-Innes, C. S. *et al.* Differential oestrogen receptor binding is associated with clinical outcome in breast cancer. *Nature* **481**, 389–393 (2012).
32. Church, D. M. *et al.* Modernizing reference genome assemblies. *PLoS Biol.* **9**, e1001091 (2011).
33. Lawrence, M. *et al.* Software for computing and annotating genomic ranges. *PLoS*

Comput. Biol. **9**, e1003118 (2013).

34. Bartlett, D. A. *et al.* High-throughput single-cell epigenomic profiling by targeted insertion of promoters (TIP-seq). *J. Cell Biol.* **220**, (2021).
35. Stadhouders, R. *et al.* Transcription regulation by distal enhancers. *Transcription* **3**, 181–186 (2012).
36. Ernst, J. & Kellis, M. Chromatin-state discovery and genome annotation with ChromHMM. *Nat. Protoc.* **12**, 2478–2492 (2017).
37. Akalin, A., Franke, V., Vlahoviček, K., Mason, C. E. & Schübeler, D. Genomation: a toolkit to summarize, annotate and visualize genomic intervals. *Bioinformatics* **31**, 1127–1129 (2015).
38. O'Leary, N. A. *et al.* Reference sequence (RefSeq) database at NCBI: current status, taxonomic expansion, and functional annotation. *Nucleic Acids Res.* **44**, D733–45 (2016).
39. Wu, T. *et al.* clusterProfiler 4.0: A universal enrichment tool for interpreting omics data. *Innovation (N Y)* **2**, 100141 (2021).
40. Heinz, S. *et al.* Simple combinations of lineage-determining transcription factors prime cis-regulatory elements required for macrophage and B cell identities. *Mol. Cell* **38**, 576–589 (2010).
41. Tanigawa, S. *et al.* Jun dimerization protein 2 is a critical component of the Nrf2/MafK complex regulating the response to ROS homeostasis. *Cell Death Dis.* **4**, e921 (2013).
42. Itoh-Nakadai, A. *et al.* The transcription repressors Bach2 and Bach1 promote B cell development by repressing the myeloid program. *Nat. Immunol.* **15**, 1171–1180 (2014).
43. Gao, J., Chen, Y.-H. & Peterson, L. C. GATA family transcriptional factors: emerging suspects in hematologic disorders. *Exp. Hematol. Oncol.* **4**, 28 (2015).
44. Lemma, R. B. *et al.* Chromatin occupancy and target genes of the haematopoietic master

transcription factor MYB. *Sci. Rep.* **11**, 9008 (2021).

45. van Arensbergen, J. *et al.* Genome-wide mapping of autonomous promoter activity in human cells. *Nat. Biotechnol.* **35**, 145–153 (2017).
46. Mews, P. *et al.* Histone methylation has dynamics distinct from those of histone acetylation in cell cycle reentry from quiescence. *Mol. Cell. Biol.* **34**, 3968–3980 (2014).
47. Gaspar, J. M. Improved peak-calling with MACS2. *bioRxiv* 496521 (2018) doi:10.1101/496521.
48. Skene, P. J. & Henikoff, S. An efficient targeted nuclease strategy for high-resolution mapping of DNA binding sites. *Elife* **6**, (2017).
49. Yashar, W. M. *et al.* GoPeaks: Histone Modification Peak Calling for CUT&Tag. *bioRxiv* 2022.01.10.475735 (2022) doi:10.1101/2022.01.10.475735.
50. Akdogan-Ozdilek, B., Duval, K. L., Meng, F. W., Murphy, P. J. & Goll, M. G. Identification of chromatin states during zebrafish gastrulation using CUT&RUN and CUT&Tag. *bioRxiv* 2021.06.22.447589 (2021) doi:10.1101/2021.06.22.447589.
51. Ernst, J. & Kellis, M. ChromHMM: automating chromatin-state discovery and characterization. *Nat. Methods* **9**, 215–216 (2012).
52. Chen, C. *et al.* Single-cell whole-genome analyses by Linear Amplification via Transposon Insertion (LIANTI). *Science* **356**, 189–194 (2017).
53. Buenrostro, J. D. *et al.* Single-cell chromatin accessibility reveals principles of regulatory variation. *Nature* **523**, 486–490 (2015).
54. Langmead, B., Trapnell, C., Pop, M. & Salzberg, S. L. Ultrafast and memory-efficient alignment of short DNA sequences to the human genome. *Genome Biol.* **10**, R25 (2009).
55. Danecek, P. *et al.* Twelve years of SAMtools and BCFtools. *Gigascience* **10**, (2021).
56. Quinlan, A. R. & Hall, I. M. BEDTools: a flexible suite of utilities for comparing genomic

features. *Bioinformatics* **26**, 841–842 (2010).

57. Burgin, J. *et al.* The European Nucleotide Archive in 2022. *Nucleic Acids Res.* (2022) doi:10.1093/nar/gkac1051.
58. Team, R. C. R: A language and environment for statistical computing (R Version 4.0. 3, R Foundation for Statistical Computing, Vienna, Austria, 2020). Preprint at (2021).
59. Ramírez, F. *et al.* deepTools2: a next generation web server for deep-sequencing data analysis. *Nucleic Acids Res.* **44**, W160–5 (2016).
60. Schep, A. N., Wu, B., Buenrostro, J. D. & Greenleaf, W. J. chromVAR: inferring transcription-factor-associated accessibility from single-cell epigenomic data. *Nat. Methods* **14**, 975–978 (2017).
61. Patel, H. *et al. nf-core/atacseq*. (Zenodo, 2022). doi:10.5281/zenodo.7384115.
62. Yu, G., Wang, L.-G. & He, Q.-Y. ChIPseeker: an R/Bioconductor package for ChIP peak annotation, comparison and visualization. *Bioinformatics* **31**, 2382–2383 (2015).
63. Carlson, M. *TxDb.Hsapiens.UCSC.hg19.knownGene*. (Bioconductor, 2015). doi:10.18129/B9.BIOC.TXDB.HSAPIENS.UCSC.HG19.KNOWNGENE.
64. Lawrence, M., Gentleman, R. & Carey, V. rtracklayer: an R package for interfacing with genome browsers. *Bioinformatics* **25**, 1841–1842 (2009).
65. Yu, G., Wang, L.-G., Han, Y. & He, Q.-Y. clusterProfiler: an R package for comparing biological themes among gene clusters. *OMICS* **16**, 284–287 (2012).

Supplementary Materials

Supplementary Tables

Sample	Total Fragments	Mapped Fragments	Alignment Rate	Duplication Rate	Unique Fragments	% chrM Fragments
Active Motif 39133 1:100 15 PCR SDS	34,467,445	34,246,137	99.36%	98.45%	531,603	9.14%
Diagenode C15410196 1:100 15 PCR SDS	13,970,902	13,884,243	99.38%	89.15%	1,506,260	11.71%
Diagenode C15410196 1:50 15 PCR SDS	90,812,784	83,771,834	92.25%	96.36%	3,051,389	3.16%
Abcam-ab177178 1:100 15 PCR SDS	7,911,303	7,839,891	99.10%	55.49%	3,489,316	0.34%
Abcam-ab4729 1:100 15 PCR SDS	146,621,482	134,760,046	91.91%	96.94%	4,123,523	1.03%
CST9733 1:100 15 PCR SDS	9,912,113	9,823,687	99.11%	57.12%	4,211,994	0.25%
H3K27ac Kaya-Okur SRR8383507 (C&T)	2,471,858	2,293,087	92.77%	20.18%	1,830,390	2.02%
H3K27ac Kaya-Okur SRR8383508 (C&T)	3,320,561	3,088,577	93.01%	14.87%	2,629,278	2.07%
H3K27ac Meers SRR8581604 (C&R)	6,777,196	5,523,031	81.49%	7.30%	5,120,026	0.10%
H3K27me3 Kaya-Okur SRR11074238 (C&T)	3,945,633	3,806,740	96.48%	1.43%	3,752,159	0.06%
H3K27me3 Kaya-Okur SRR11074239 (C&T)	4,159,984	4,051,439	97.39%	1.36%	3,996,319	0.04%
H3K27me3 Meers SRR9073702 (C&R)	9,047,596	8,668,833	95.81%	1.58%	8,531,865	0.02%
Active Motif 39133 1:100 11 PCR SDS	4,380,560	4,347,855	99.25%	81.68%	796,514	6.39%
Diagenode C15410196 1:50 11 PCR SDS	6,379,299	6,315,402	99.00%	85.67%	904,726	8.45%
Abcam-ab177178 1:100 11 PCR SDS	21,349,457	21,233,210	99.46%	82.97%	3,615,527	0.59%
Abcam-ab4729 1:100 11 PCR SDS	9,195,139	9,136,507	99.36%	80.53%	1,779,088	2.58%
H3K27me3 11 PCR SDS	17,976,126	17,862,415	99.37%	88.75%	2,009,039	1.50%
Active Motif 39133 1:100 11 PCR column	1,475,470	1,464,695	99.27%	46.33%	786,081	7.70%
Diagenode C15410196 1:50 11 PCR column	1,800,855	1,785,868	99.17%	52.74%	843,989	12.40%
Abcam-ab177178 1:100 11 PCR column	2,733,847	2,713,351	99.25%	51.59%	1,313,493	1.70%
Abcam-ab4729 1:100 11 PCR column	2,153,420	2,140,283	99.39%	51.21%	1,044,240	2.73%
H3K27me3 11 PCR column	3,594,729	3,563,911	99.14%	48.88%	1,822,039	1.64%
Abcam-ab177178 1:100 13 PCR SDS	8,521,987	8,436,844	99.00%	73.70%	2,219,025	0.66%
Abcam-ab4729 1:100 13 PCR SDS	10,601,213	10,513,132	99.17%	85.88%	1,484,538	2.29%
Active Motif 39133 1:100 13 PCR SDS	9,424,194	9,368,250	99.41%	83.89%	1,508,766	12.90%
CST9733 1:100 13 PCR SDS	25,021,566	24,909,845	99.55%	84.24%	3,926,215	0.54%
Diagenode C15410196 1:50 13 PCR SDS	9,497,265	9,431,247	99.30%	79.54%	1,929,369	9.76%
Abcam-ab177178 1:100 13 PCR column	10,658,973	10,607,882	99.52%	77.48%	2,389,150	0.55%
Abcam-ab4729 1:100 13 PCR column	4,908,403	4,878,543	99.39%	81.33%	910,834	2.10%
Active Motif 39133 1:100 13 PCR column	5,617,892	5,575,622	99.25%	87.05%	722,071	12.54%
CST9733 1:100 13 PCR column	14,268,256	14,197,536	99.50%	82.79%	2,442,942	0.98%

Diagenode C15410196 1:50 13 PCR column	5,168,457	5,110,735	98.88%	85.17%	758,019	16.85%
Diagenode C15410196 1:100 15 PCR SDS TSA	3,157,488	3,133,254	99.23%	75.22%	776,367	1.65%
Diagenode C15410196 1:50 15 PCR SDS TSA	3,922,942	3,879,429	98.89%	70.88%	1,129,659	8.98%
Abcam-ab177178 1:100 15 PCR SDS TSA	5,178,780	5,132,446	99.11%	77.70%	1,144,541	8.61%
Abcam-ab4729 1:100 15 PCR SDS TSA	12,570,714	12,473,438	99.23%	64.56%	4,420,973	0.71%

Supplementary Table 1. Sequencing and alignment results of all CUT&Tag and CUT&RUN data.

Sample	Peaks called			
	SEACR		MACS2	
	No duplicates	With duplicates	No duplicates	With duplicates
Active Motif	2,497	3,005	1,762	95,223
Diagenode (1:100)	7,065	7,570	6,717	180,149
Diagenode (1:50)	11,094	11,364	19,672	167,500
Abcam-ab177178	15,458	15,838	9,688	93,453
Abcam-ab4729	12,657	12,924	24,076	275,284
H3K27me3	103,953	104,914	86,965	219,783
H3K27ac Kaya-Okur SRR8383507 (C&T)	6,415	6,451	12,922	18,105
H3K27ac Kaya-Okur SRR8383508 (C&T)	8,044	8,076	18,190	22,789
H3K27ac Meers SRR8581604 (C&R)	16,974	16,983	20,589	23,325
H3K27me3 Kaya-Okur SRR11074238 (C&T)	115,643	115,627	81,134	83,054
H3K27me3 Kaya-Okur SRR11074239 (C&T)	117,329	117,282	87,095	89,009
H3K27me3 Meers SRR9073702 (C&R)	100,777	100,842	81,465	82,758

Supplementary Table 2. Numbers of peaks called with SEACR and MACS2 under different conditions, after filtering out blacklisted peaks.

Sample	Recall +chrM	Recall - chrM	Precision +chrM	Precision - chrM
Abcam-ab4729	46.5%	45.9%	85.2%	89.7%
Abcam-ab177178	25.4%	25.1%	57.2%	61.8%
Active Motif	4.7%	4.6%	61.6%	77.2%

Supplementary Table 3. ENCODE H3K27ac peak capture metrics with vs without mitochondrial reads retained prior to peak calling for select samples, after removing all peaks on non-standard chromosomes.

Supplementary Figures

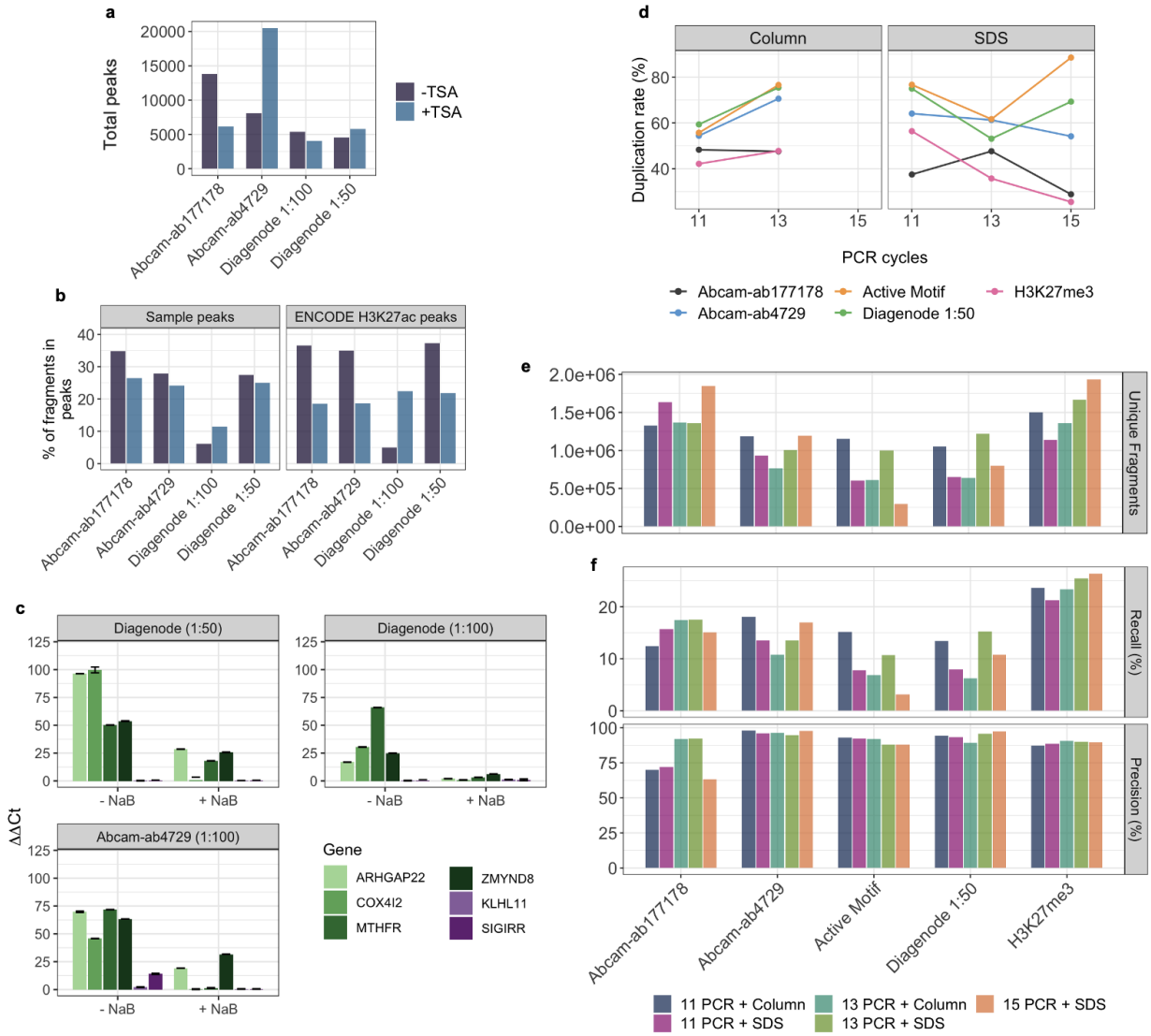

Supplementary Figure 1. Experimental optimization of CUT&Tag. a, Total SEACR peaks called and **b**, FRiP scores obtained (in both called sample peaks and ENCODE H3K27ac peaks) with and without treatment with TSA; **c**, Results of qPCR amplification of genes in most significant ENCODE H3K27ac peak regions (positive controls; green) versus least significant (negative controls; purple) in CUT&Tag experiments performed with top-performing antibodies, with and without HDAC inhibitor sodium butyrate (NaB; 5 mM); **d**, Duplication rates, **e**, total unique fragments, and **f**, ENCODE capture metrics obtained using column- or SDS-based DNA extraction and 11, 13 or 15 PCR cycles for sequencing library preparation, with all samples downsampled to the same read depth of 2.6 million paired-end reads

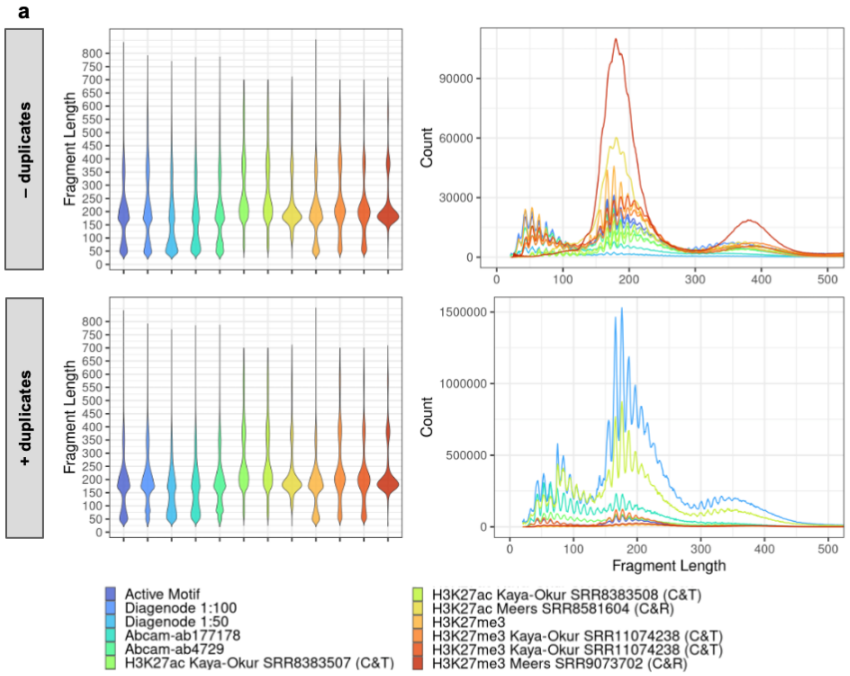
a
– duplicates
+ duplicates
Fragment Length
Count
Fragment Length
Active Motif
Diagenode 1:100
Diagenode 1:50
Abcam-ab177178
Abcam-ab4729
H3K27ac Kaya-Okur SRR8383507 (C&T)
H3K27ac Kaya-Okur SRR8383508 (C&T)
H3K27ac Meers SRR8581604 (C&R)
H3K27me3
H3K27me3 Kaya-Okur SRR11074238 (C&T)
H3K27me3 Kaya-Okur SRR11074238 (C&T)
H3K27me3 Meers SRR9073702 (C&R)

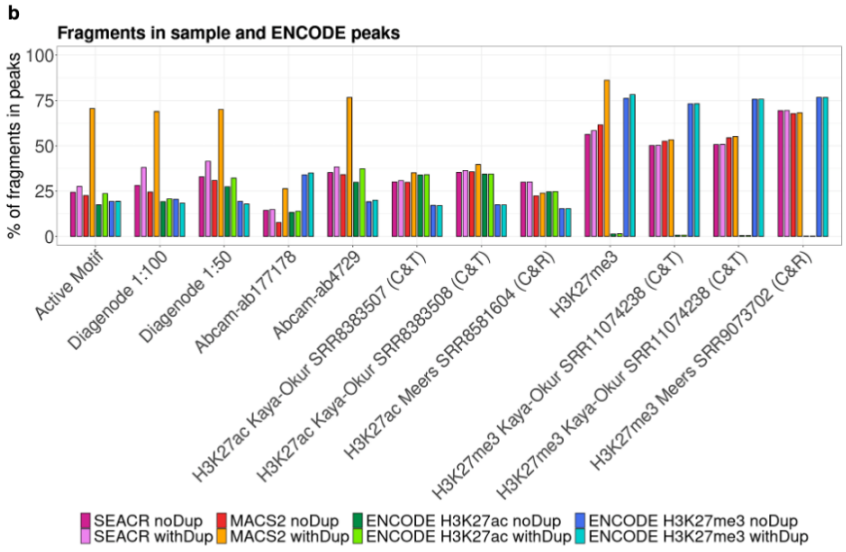
b
Fragments in sample and ENCODE peaks
% of fragments in peaks
Active Motif
Diagenode 1:100
Diagenode 1:50
Abcam-ab177178
Abcam-ab4729
H3K27ac Kaya-Okur SRR8383507 (C&T)
H3K27ac Kaya-Okur SRR8383508 (C&T)
H3K27ac Meers SRR8581604 (C&R)
H3K27me3
H3K27me3 Kaya-Okur SRR11074238 (C&T)
H3K27me3 Kaya-Okur SRR11074238 (C&T)
H3K27me3 Meers SRR9073702 (C&R)
SEACR noDup
SEACR withDup
MACS2 noDup
MACS2 withDup
ENCODE H3K27ac noDup
ENCODE H3K27ac withDup
ENCODE H3K27me3 noDup
ENCODE H3K27me3 withDup

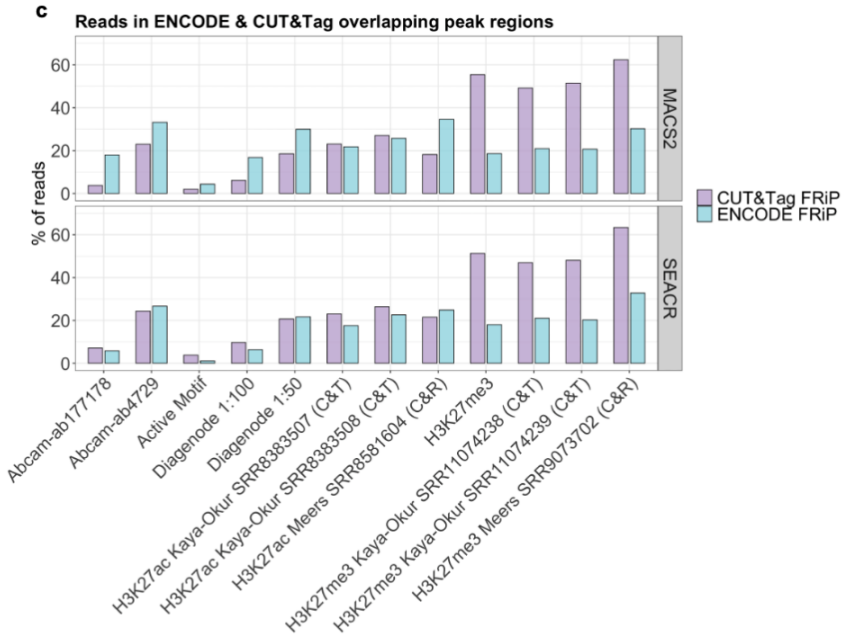
c
Reads in ENCODE & CUT&Tag overlapping peak regions
% of reads
MACS2
SEACR
CUT&Tag FRiP
ENCODE FRiP
Abcam-ab177178
Abcam-ab4729
Active Motif
Diagenode 1:100
Diagenode 1:50
H3K27ac Kaya-Okur SRR8383507 (C&T)
H3K27ac Kaya-Okur SRR8383508 (C&T)
H3K27ac Meers SRR8581604 (C&R)
H3K27me3
H3K27me3 Kaya-Okur SRR11074238 (C&T)
H3K27me3 Kaya-Okur SRR11074239 (C&T)
H3K27me3 Meers SRR9073702 (C&R)

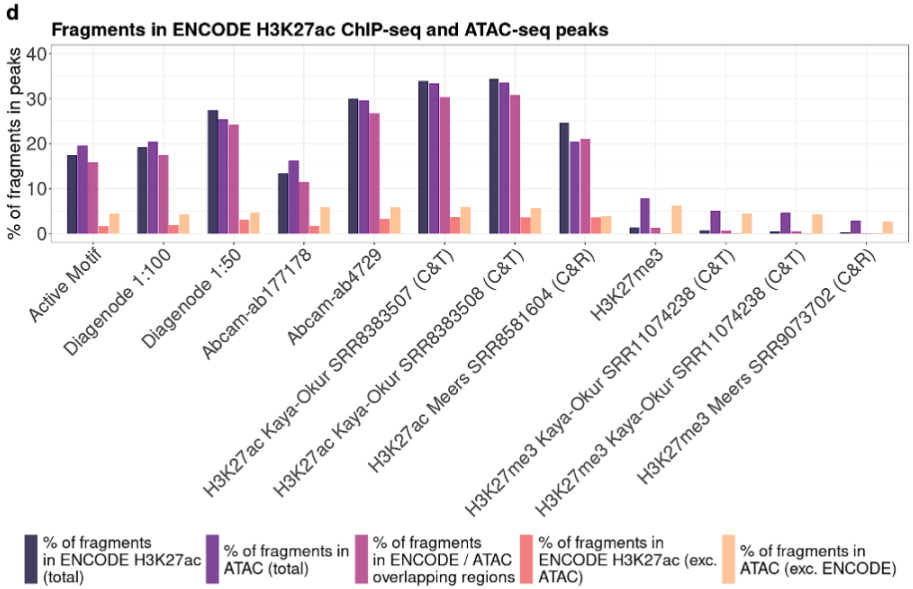
d
Fragments in ENCODE H3K27ac ChIP-seq and ATAC-seq peaks
% of fragments in peaks
Active Motif
Diagenode 1:100
Diagenode 1:50
Abcam-ab177178
Abcam-ab4729
H3K27ac Kaya-Okur SRR8383507 (C&T)
H3K27ac Kaya-Okur SRR8383508 (C&T)
H3K27ac Meers SRR8581604 (C&R)
H3K27me3
H3K27me3 Kaya-Okur SRR11074238 (C&T)
H3K27me3 Kaya-Okur SRR11074238 (C&T)
H3K27me3 Meers SRR9073702 (C&R)
% of fragments in ENCODE H3K27ac (total)
% of fragments in ATAC (total)
% of fragments in ENCODE / ATAC overlapping regions
% of fragments in ENCODE H3K27ac (exc. ATAC)
% of fragments in ATAC (exc. ENCODE)

Supplementary Figure 2. a, Fragment length distributions; **b**, Percentages of reads in peaks called with SEACR or MACS2, with or without duplicates, as well as ENCODE H3K27ac ChIP-seq narrow peaks and ENCODE H3K27me3 ChIP-seq broad peaks; **c**, Percentages of CUT&Tag and ENCODE ChIP-seq reads in overlapping ENCODE and CUT&Tag peak regions; **d**, Percentages of sample reads in ENCODE H3K27ac ChIP-seq and ATAC-seq peaks. Figures have been expanded to include all analyzed samples and published datasets.

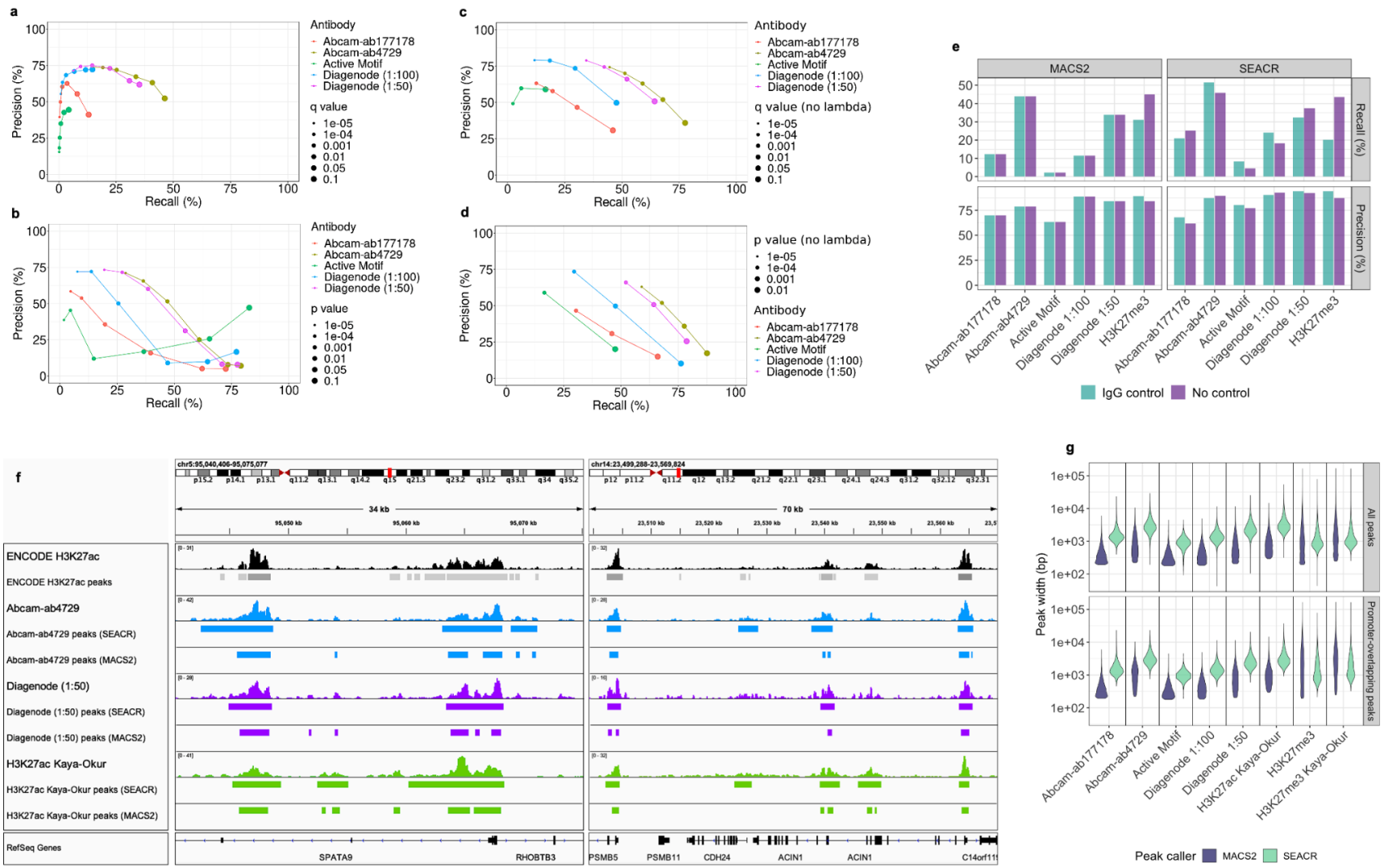
a
Precision (%)
Recall (%)
Antibody
Abcam-ab177178
Abcam-ab4729
Active Motif
Diagenode (1:100)
Diagenode (1:50)
q value
1e-05
1e-04
0.001
0.01
0.05
0.1
b
p value
c
q value (no lambda)
d
p value (no lambda)
e
MACS2
SEACR
Recall (%)
Precision (%)
IgG control
No control
f
ENCODE H3K27ac
ENCODE H3K27ac peaks
Abcam-ab4729
Abcam-ab4729 peaks (SEACR)
Abcam-ab4729 peaks (MACS2)
Diagenode (1:50)
Diagenode (1:50) peaks (SEACR)
Diagenode (1:50) peaks (MACS2)
H3K27ac Kaya-Okur
H3K27ac Kaya-Okur peaks (SEACR)
H3K27ac Kaya-Okur peaks (MACS2)
RefSeq Genes
SPATA9
RHOBTB3
PSMB5
PSMB11
CDH24
ACIN1
g
Peak width (bp)
All peaks
Promoter-overlapping peaks
Abcam-ab177178
Abcam-ab4729
Active Motif
Diagenode 1:100
Diagenode 1:50
H3K27ac Kaya-Okur
H3K27me3
H3K27me3 Kaya-Okur
Peak caller
MACS2
SEACR

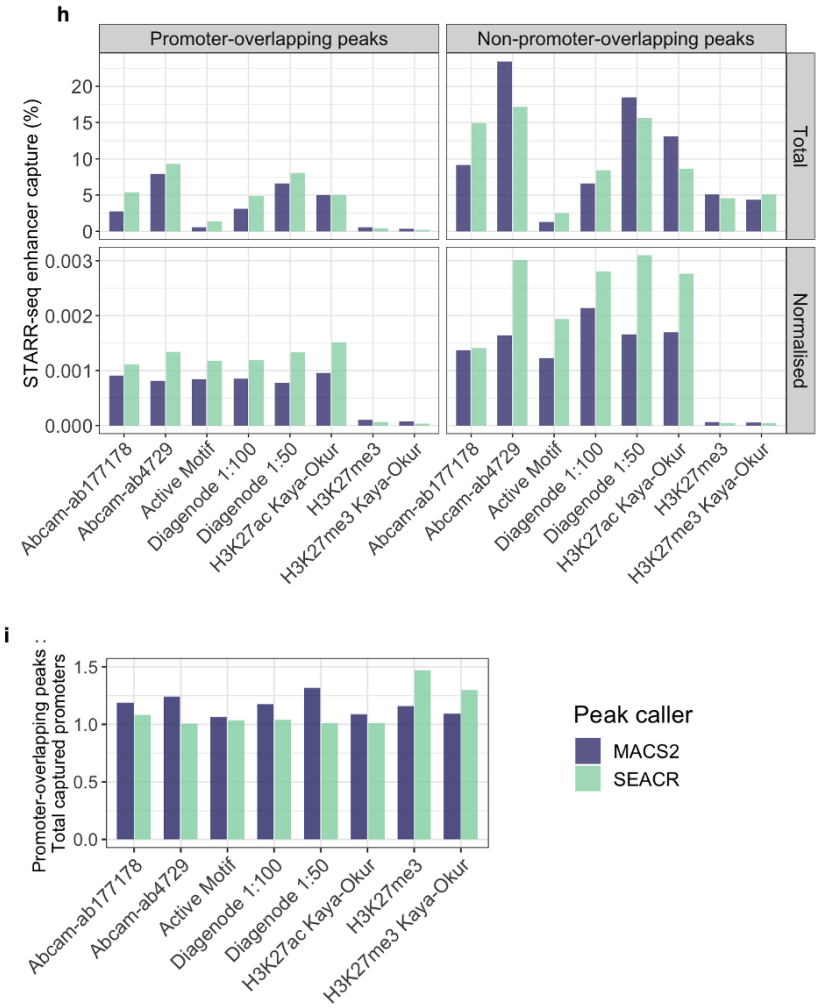

Supplementary Figure 3. Optimization of peak calling with MACS2, showing precision vs recall when varying **a**, q value; **b**, p value; **c**, q value with local lambda deactivated; **d**, p value with local lambda deactivated. **e**, Precision and recall of ENCODE capture with and without an IgG control; **f**, IGV snapshots showing examples of SEACR and MACS2 peaks for top H3K27ac CUT&Tag samples; **g**, violin plots showing width distributions of all and promoter-overlapping SEACR and MACS2 peaks, where the promoter region was taken to be +/-1.5kb about the promoter; **h**, capture of accessible STARR-seq enhancers by promoter-overlapping and non-promoter-overlapping SEACR and MACS2 sample peaks, as an unadjusted percentage (top), and percentage normalized by total sample peak number (bottom); **i**, average numbers of SEACR and MACS2 peaks per captured promoter.

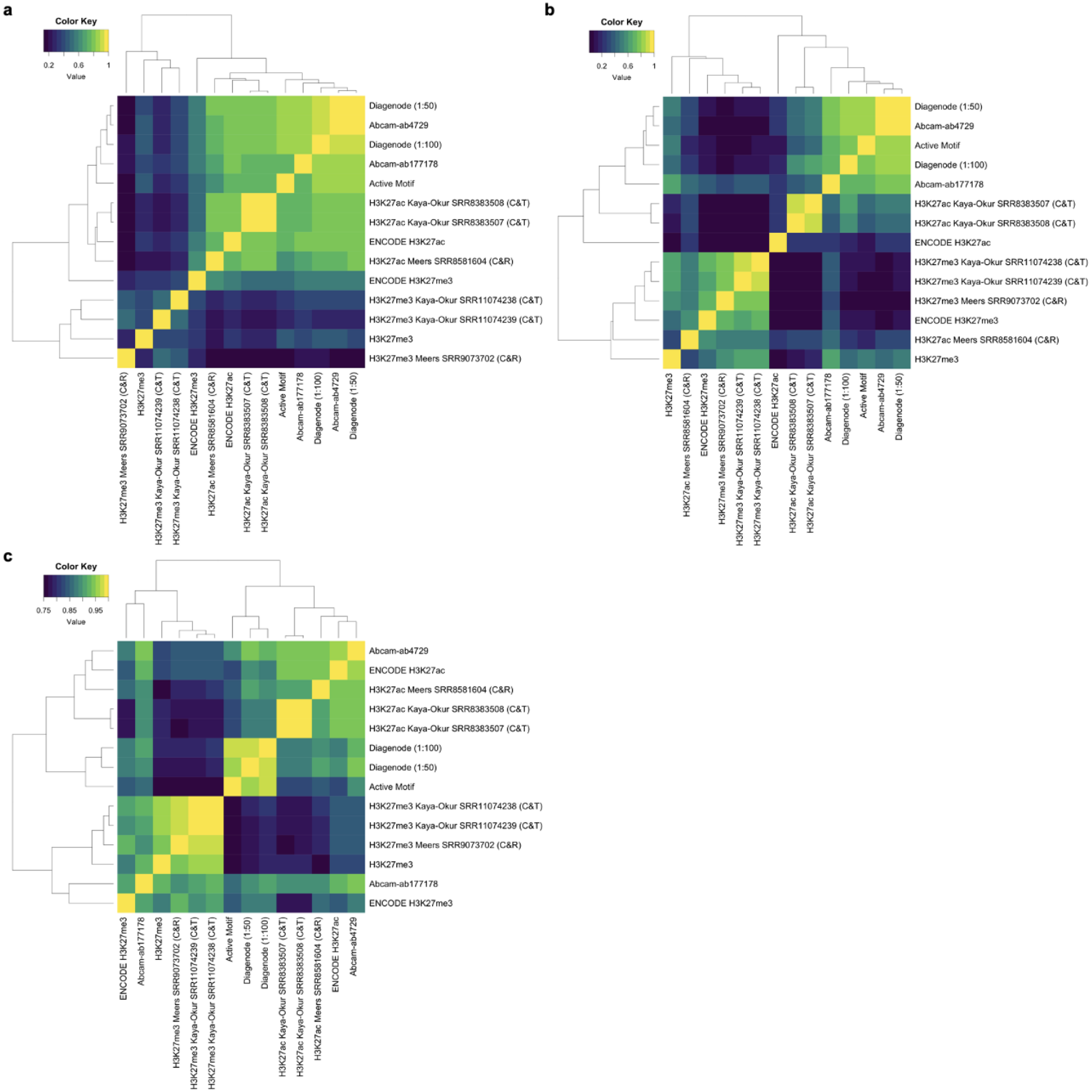
a
Color Key
0.2
0.6
1
Value
Diagenode (1:50)
Abcam-ab4729
Diagenode (1:100)
Abcam-ab177178
Active Motif
H3K27ac Kaya-Okur SRR8383508 (C&T)
H3K27ac Kaya-Okur SRR8383507 (C&T)
ENCODE H3K27ac
H3K27ac Meers SRR8581604 (C&R)
ENCODE H3K27me3
H3K27me3 Kaya-Okur SRR11074238 (C&T)
H3K27me3 Kaya-Okur SRR11074239 (C&T)
H3K27me3
H3K27me3 Meers SRR9073702 (C&R)
b
Color Key
0.2
0.6
1
Value
Diagenode (1:50)
Abcam-ab4729
Active Motif
Diagenode (1:100)
Abcam-ab177178
H3K27ac Kaya-Okur SRR8383507 (C&T)
H3K27ac Kaya-Okur SRR8383508 (C&T)
ENCODE H3K27ac
H3K27me3 Kaya-Okur SRR11074238 (C&T)
H3K27me3 Kaya-Okur SRR11074239 (C&T)
H3K27me3 Meers SRR9073702 (C&R)
ENCODE H3K27me3
H3K27ac Meers SRR8581604 (C&R)
H3K27me3
c
Color Key
0.75
0.85
0.95
Value
Abcam-ab4729
ENCODE H3K27ac
H3K27ac Meers SRR8581604 (C&R)
H3K27ac Kaya-Okur SRR8383508 (C&T)
H3K27ac Kaya-Okur SRR8383507 (C&T)
Diagenode (1:100)
Diagenode (1:50)
Active Motif
H3K27me3 Kaya-Okur SRR11074238 (C&T)
H3K27me3 Kaya-Okur SRR11074239 (C&T)
H3K27me3 Meers SRR9073702 (C&R)
H3K27me3
Abcam-ab177178
ENCODE H3K27me3

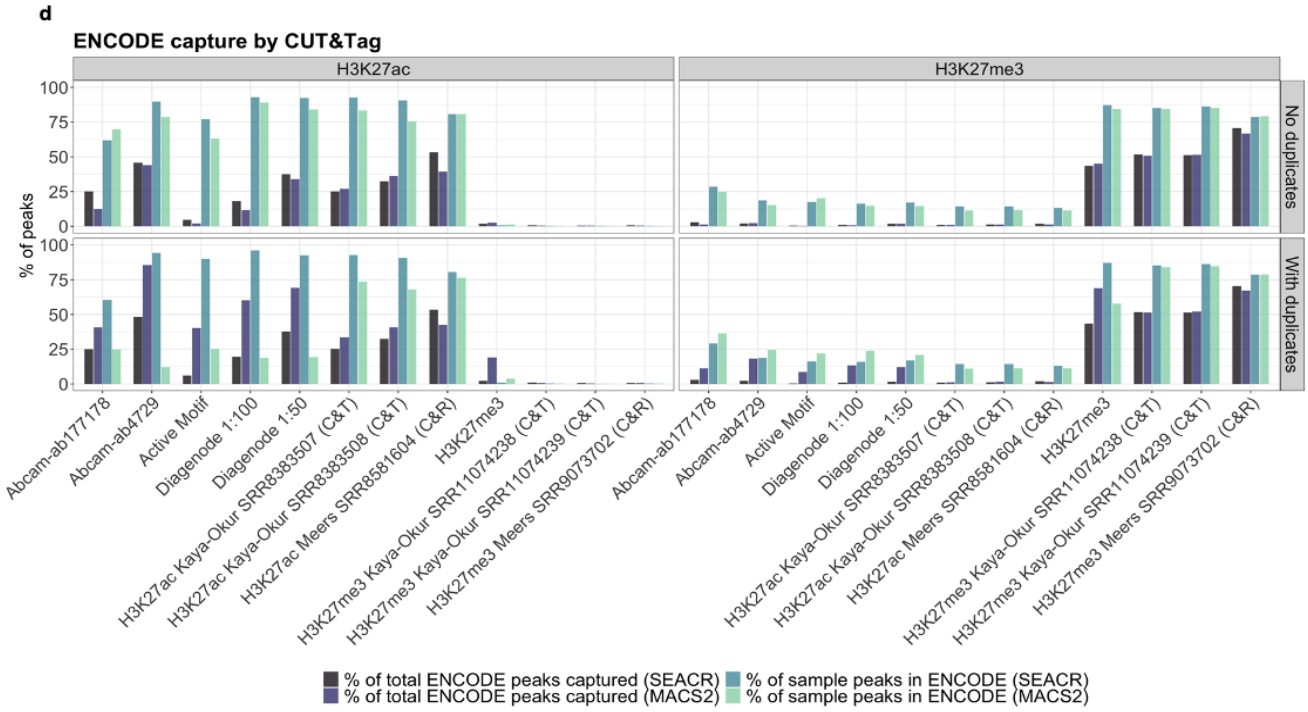
d
ENCODE capture by CUT&Tag
H3K27ac
H3K27me3
No duplicates
With duplicates
% of peaks
Abcam-ab177178
Abcam-ab4729
Active Motif
Diagenode 1:100
Diagenode 1:50
H3K27ac Kaya-Okur SRR8383507 (C&T)
H3K27ac Kaya-Okur SRR8383508 (C&T)
H3K27ac Meers SRR8581604 (C&R)
H3K27me3
H3K27me3 Kaya-Okur SRR11074238 (C&T)
H3K27me3 Kaya-Okur SRR11074239 (C&T)
H3K27me3 Meers SRR9073702 (C&R)
% of total ENCODE peaks captured (SEACR)
% of total ENCODE peaks captured (MACS2)
% of sample peaks in ENCODE (SEACR)
% of sample peaks in ENCODE (MACS2)

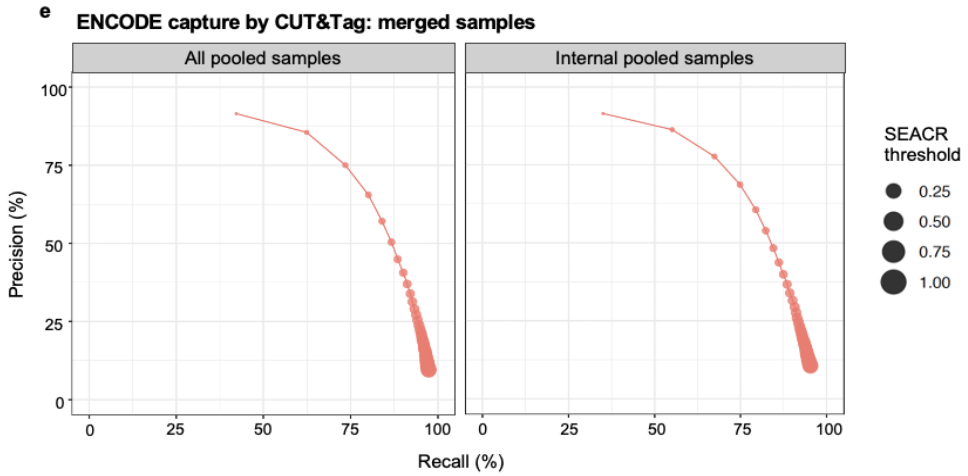
e
ENCODE capture by CUT&Tag: merged samples
All pooled samples
Internal pooled samples
Precision (%)
Recall (%)
SEACR threshold
0.25
0.50
0.75
1.00

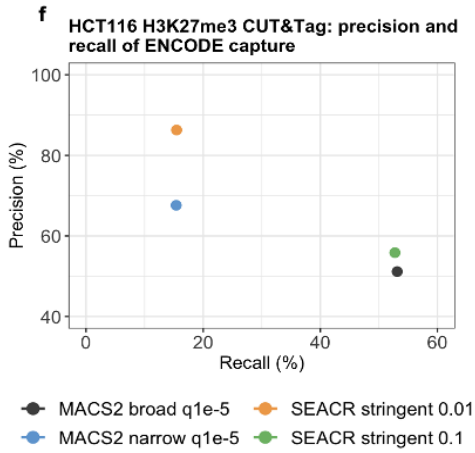
f
HCT116 H3K27me3 CUT&Tag: precision and recall of ENCODE capture
Precision (%)
Recall (%)
MACS2 broad q1e-5
MACS2 narrow q1e-5
SEACR stringent 0.01
SEACR stringent 0.1

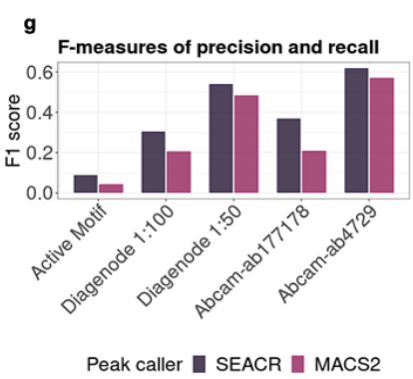
g
F-measures of precision and recall
F1 score
Active Motif
Diagenode 1:100
Diagenode 1:50
Abcam-ab177178
Abcam-ab4729
Peak caller
SEACR
MACS2

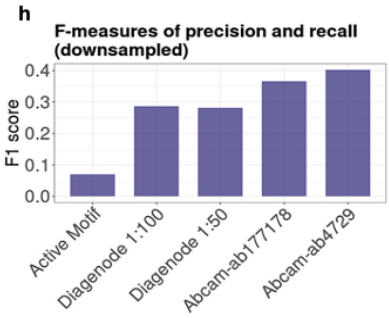
h
F-measures of precision and recall (downsampled)
F1 score
Active Motif
Diagenode 1:100
Diagenode 1:50
Abcam-ab177178
Abcam-ab4729

Supplementary Figure 4. Read correlations across **a**, ENCODE H3K27ac ChIP-seq peak ranges, **b**, 500bp genome-wide bins and **c**, ENCODE H3K27me3 ChIP-seq peak ranges; **d**, capture of ENCODE H3K27ac and H3K27me3 ChIP-seq peaks by CUT&Tag and CUT&RUN peaks called with SEACR or MACS2, with or without duplicates; **e**, precision and recall of ENCODE capture with an aggregate sample comprising all internal and published CUT&Tag samples (left) or just internal samples (right), using different SEACR thresholds (between 0.01 and 1) for calling pooled peaks; **f**, precision and recall of ENCODE H3K27me3 peak capture in the HCT116 cell line; F-measures of precision and recall of tested H3K27ac antibodies at **g**, maximum read depth and **h**, 8 million paired-end reads each. Figures have been expanded to include all analysed samples and published datasets.

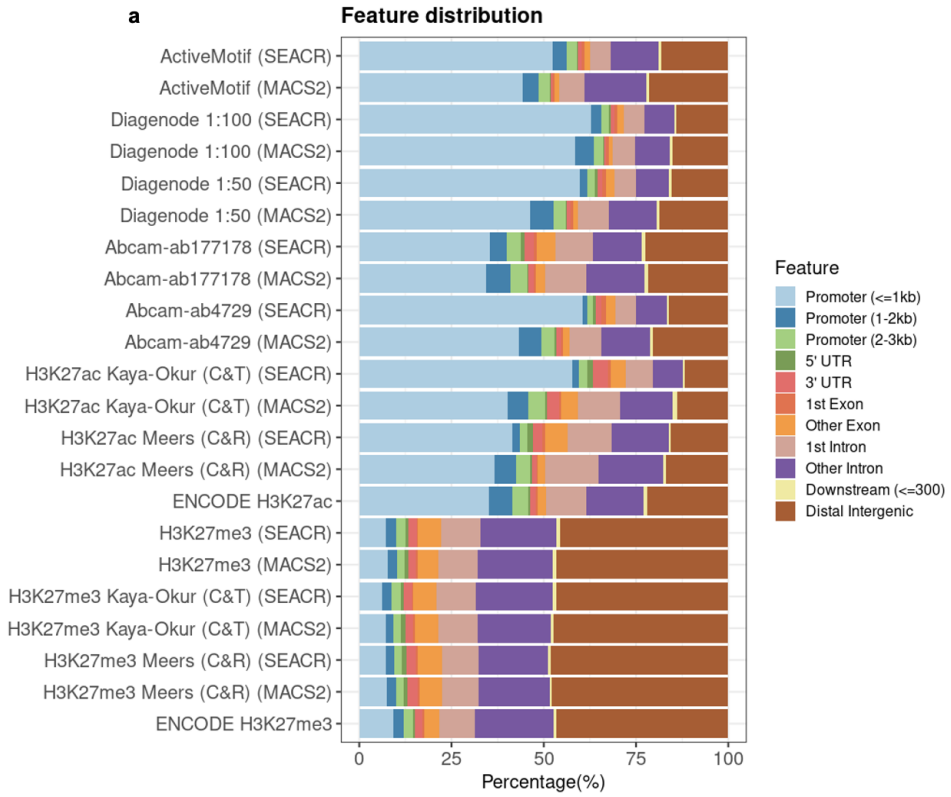
a
Feature distribution
ActiveMotif (SEACR)
ActiveMotif (MACS2)
Diagenode 1:100 (SEACR)
Diagenode 1:100 (MACS2)
Diagenode 1:50 (SEACR)
Diagenode 1:50 (MACS2)
Abcam-ab177178 (SEACR)
Abcam-ab177178 (MACS2)
Abcam-ab4729 (SEACR)
Abcam-ab4729 (MACS2)
H3K27ac Kaya-Okur (C&T) (SEACR)
H3K27ac Kaya-Okur (C&T) (MACS2)
H3K27ac Meers (C&R) (SEACR)
H3K27ac Meers (C&R) (MACS2)
ENCODE H3K27ac
H3K27me3 (SEACR)
H3K27me3 (MACS2)
H3K27me3 Kaya-Okur (C&T) (SEACR)
H3K27me3 Kaya-Okur (C&T) (MACS2)
H3K27me3 Meers (C&R) (SEACR)
H3K27me3 Meers (C&R) (MACS2)
ENCODE H3K27me3
0
25
50
75
100
Percentage(%)
Feature
Promoter (<=1kb)
Promoter (1-2kb)
Promoter (2-3kb)
5' UTR
3' UTR
1st Exon
Other Exon
1st Intron
Other Intron
Downstream (<=300)
Distal Intergenic

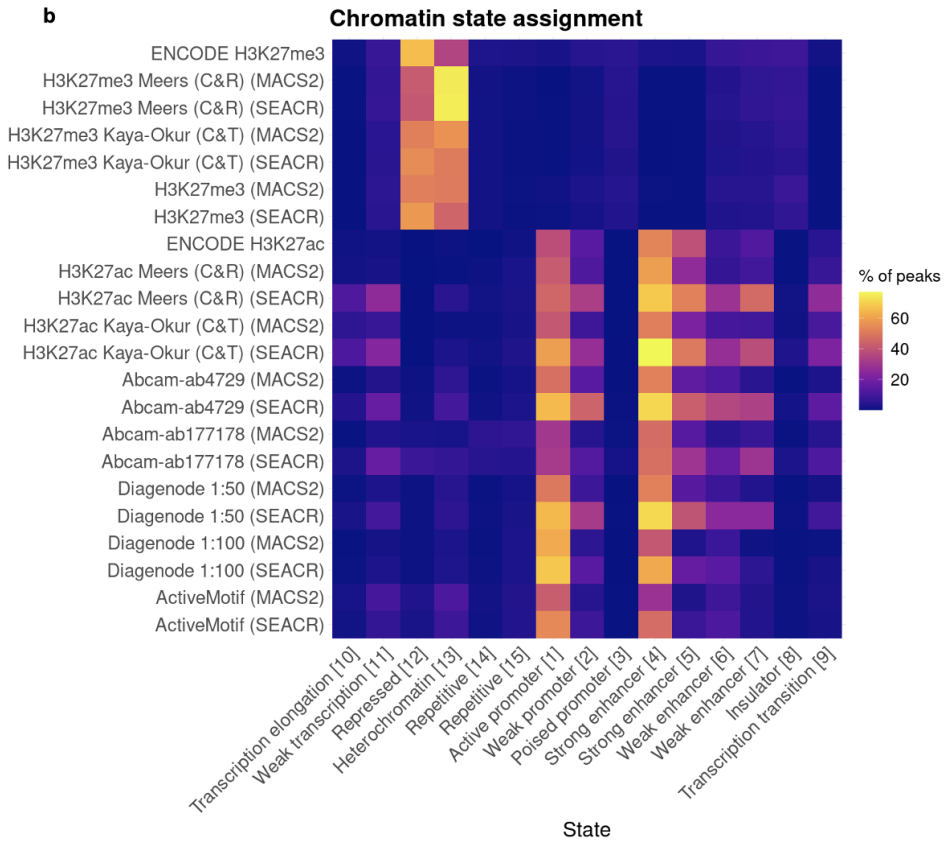
b
Chromatin state assignment
ENCODE H3K27me3
H3K27me3 Meers (C&R) (MACS2)
H3K27me3 Meers (C&R) (SEACR)
H3K27me3 Kaya-Okur (C&T) (MACS2)
H3K27me3 Kaya-Okur (C&T) (SEACR)
H3K27me3 (MACS2)
H3K27me3 (SEACR)
ENCODE H3K27ac
H3K27ac Meers (C&R) (MACS2)
H3K27ac Meers (C&R) (SEACR)
H3K27ac Kaya-Okur (C&T) (MACS2)
H3K27ac Kaya-Okur (C&T) (SEACR)
Abcam-ab4729 (MACS2)
Abcam-ab4729 (SEACR)
Abcam-ab177178 (MACS2)
Abcam-ab177178 (SEACR)
Diagenode 1:50 (MACS2)
Diagenode 1:50 (SEACR)
Diagenode 1:100 (MACS2)
Diagenode 1:100 (SEACR)
ActiveMotif (MACS2)
ActiveMotif (SEACR)
Transcription elongation [10]
Weak transcription [11]
Repressed [12]
Heterochromatin [13]
Repetitive [14]
Repetitive [15]
Active promoter [1]
Weak promoter [2]
Poised promoter [3]
Strong enhancer [4]
Strong enhancer [5]
Weak enhancer [6]
Weak enhancer [7]
Insulator [8]
Transcription transition [9]
State
% of peaks
60
40
20

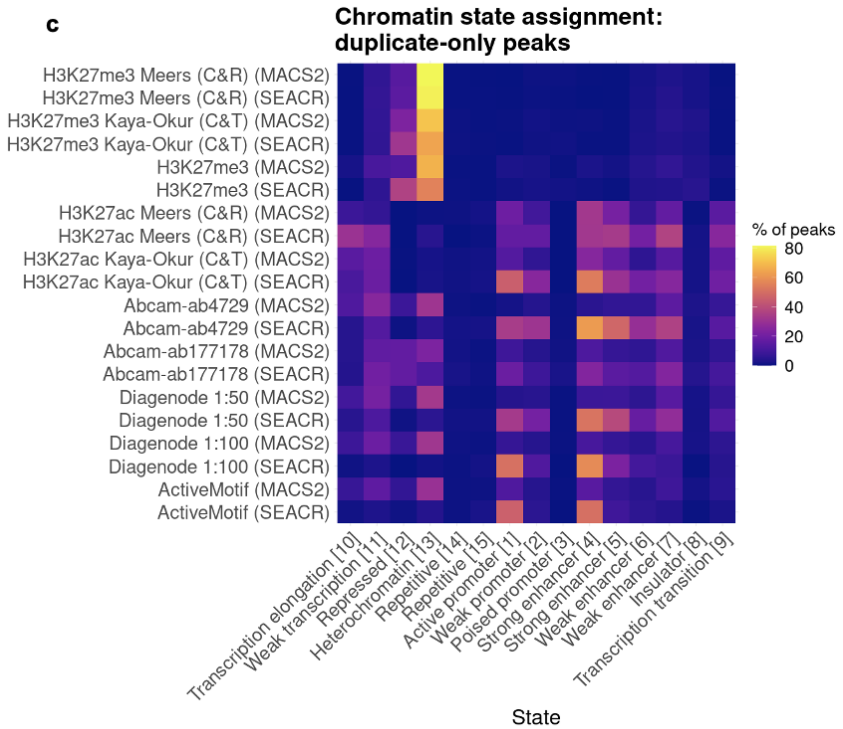
c
Chromatin state assignment:
duplicate-only peaks
H3K27me3 Meers (C&R) (MACS2)
H3K27me3 Meers (C&R) (SEACR)
H3K27me3 Kaya-Okur (C&T) (MACS2)
H3K27me3 Kaya-Okur (C&T) (SEACR)
H3K27me3 (MACS2)
H3K27me3 (SEACR)
H3K27ac Meers (C&R) (MACS2)
H3K27ac Meers (C&R) (SEACR)
H3K27ac Kaya-Okur (C&T) (MACS2)
H3K27ac Kaya-Okur (C&T) (SEACR)
Abcam-ab4729 (MACS2)
Abcam-ab4729 (SEACR)
Abcam-ab177178 (MACS2)
Abcam-ab177178 (SEACR)
Diagenode 1:50 (MACS2)
Diagenode 1:50 (SEACR)
Diagenode 1:100 (MACS2)
Diagenode 1:100 (SEACR)
ActiveMotif (MACS2)
ActiveMotif (SEACR)
Transcription elongation [10]
Weak transcription [11]
Repressed [12]
Heterochromatin [13]
Repetitive [14]
Repetitive [15]
Active promoter [1]
Weak promoter [2]
Poised promoter [3]
Strong enhancer [4]
Strong enhancer [5]
Weak enhancer [6]
Weak enhancer [7]
Insulator [8]
Transcription transition [9]
State
% of peaks
80
60
40
20
0

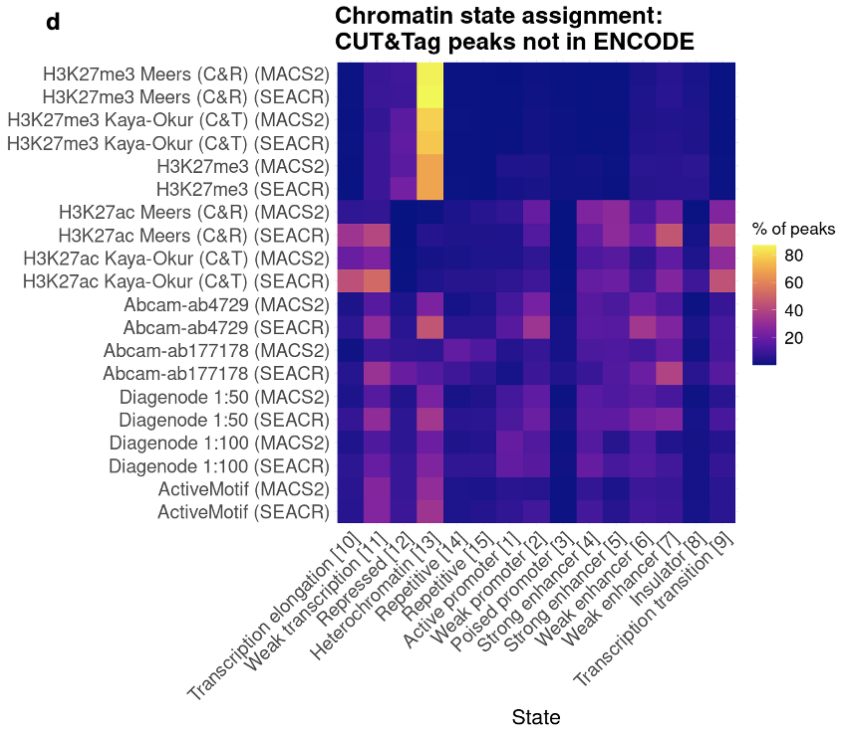
d
Chromatin state assignment:
CUT&Tag peaks not in ENCODE
H3K27me3 Meers (C&R) (MACS2)
H3K27me3 Meers (C&R) (SEACR)
H3K27me3 Kaya-Okur (C&T) (MACS2)
H3K27me3 Kaya-Okur (C&T) (SEACR)
H3K27me3 (MACS2)
H3K27me3 (SEACR)
H3K27ac Meers (C&R) (MACS2)
H3K27ac Meers (C&R) (SEACR)
H3K27ac Kaya-Okur (C&T) (MACS2)
H3K27ac Kaya-Okur (C&T) (SEACR)
Abcam-ab4729 (MACS2)
Abcam-ab4729 (SEACR)
Abcam-ab177178 (MACS2)
Abcam-ab177178 (SEACR)
Diagenode 1:50 (MACS2)
Diagenode 1:50 (SEACR)
Diagenode 1:100 (MACS2)
Diagenode 1:100 (SEACR)
ActiveMotif (MACS2)
ActiveMotif (SEACR)
Transcription elongation [10]
Weak transcription [11]
Repressed [12]
Heterochromatin [13]
Repetitive [14]
Repetitive [15]
Active promoter [1]
Weak promoter [2]
Poised promoter [3]
Strong enhancer [4]
Strong enhancer [5]
Weak enhancer [6]
Weak enhancer [7]
Insulator [8]
Transcription transition [9]
State
% of peaks
80
60
40
20

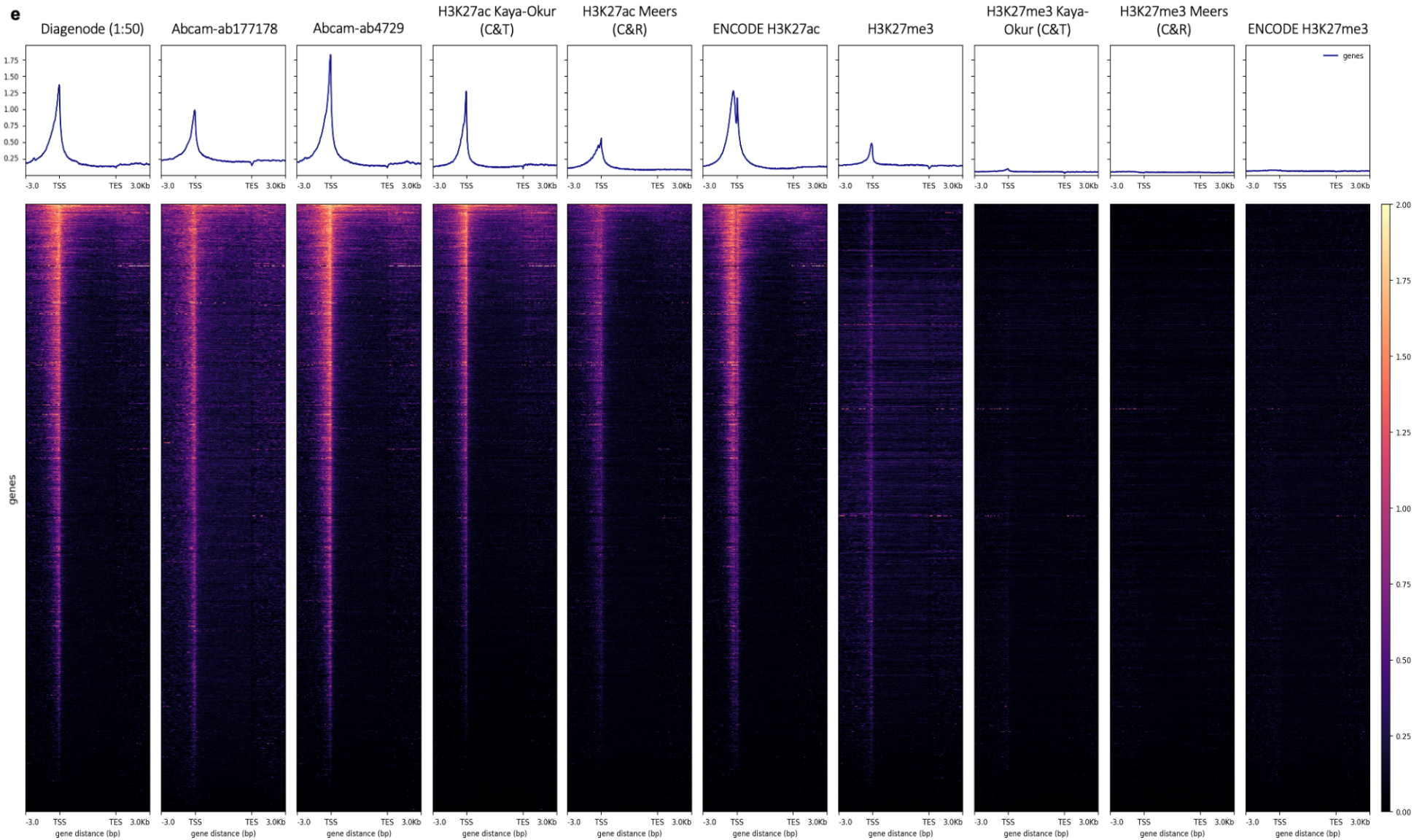
e
Diagenode (1:50)
Abcam-ab177178
Abcam-ab4729
H3K27ac Kaya-Okur (C&T)
H3K27ac Meers (C&R)
ENCODE H3K27ac
H3K27me3
H3K27me3 Kaya-Okur (C&T)
H3K27me3 Meers (C&R)
ENCODE H3K27me3
genes
-3.0 TSS TES 3.0Kb
gene distance (bp)
2.00
1.75
1.50
1.25
1.00
0.75
0.50
0.25
0.00

Supplementary Figure 5. a, Regulatory element assignment to CUT&Tag, CUT&RUN, and ENCODE peaks. Chromatin state assignments of: **b**, all peaks, called with SEACR or MACS2, **c**, CUT&Tag peaks specific to duplicate-containing samples, **d**, CUT&Tag peaks not in ENCODE H3K27ac. **e**, Heatmaps showing average read coverage around hg19 transcription start sites, with all samples subsampled to 2 million reads. Figures have been expanded to include all analyzed samples and published datasets.

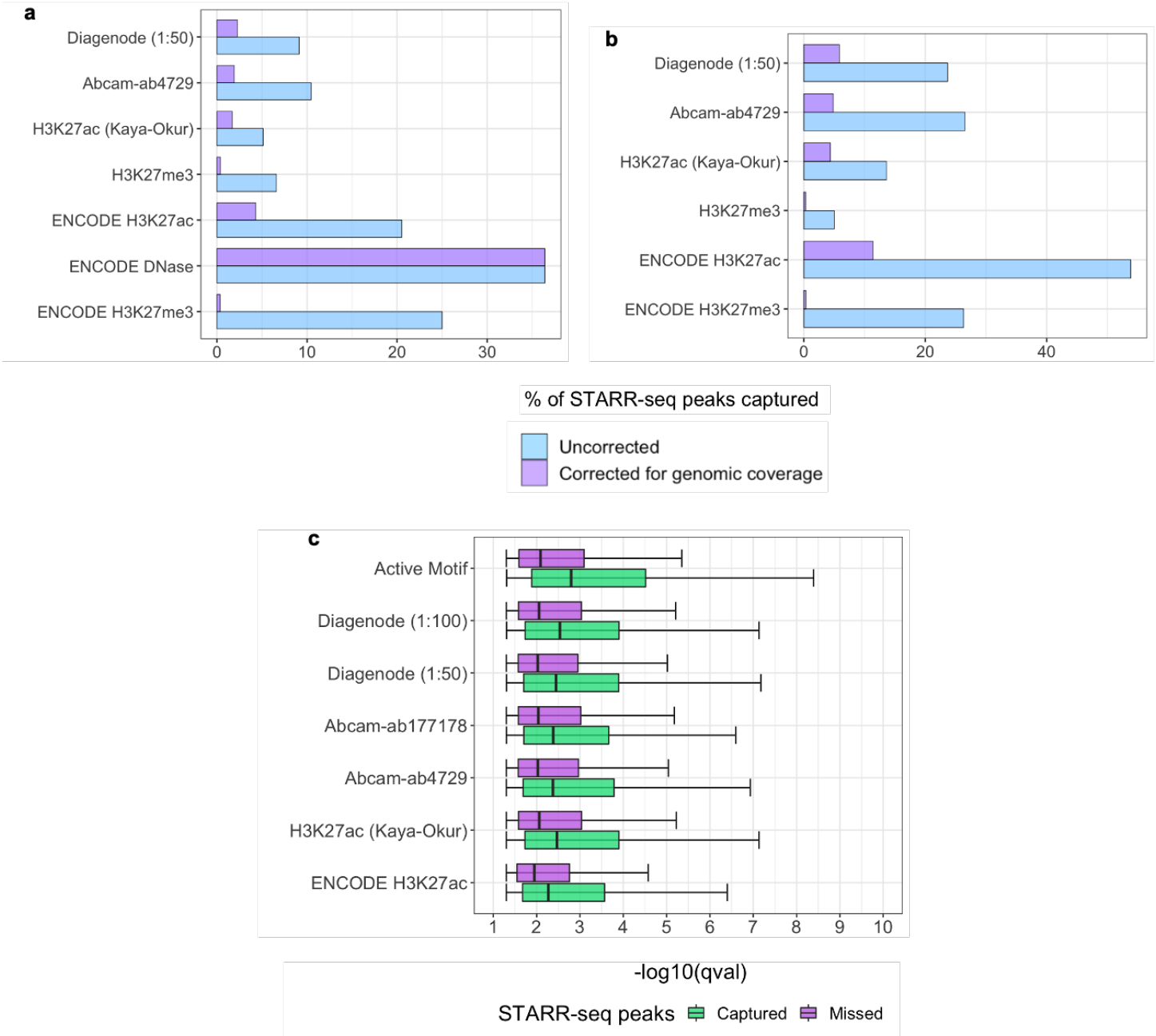

Supplementary Figure 6. Capture of **a**, genome-wide STARR-seq enhancers and **b**, STARR-seq enhancers overlapping with ENCODE K562 DNase-seq peaks by CUT&Tag (SEACR; deduplicated) and ENCODE datasets; **c**, comparison of -log10(q) values of DNase-overlapping STARR-seq peaks captured and not captured by CUT&Tag and ChIP-seq. Whiskers correspond to 1.5 * the IQR.

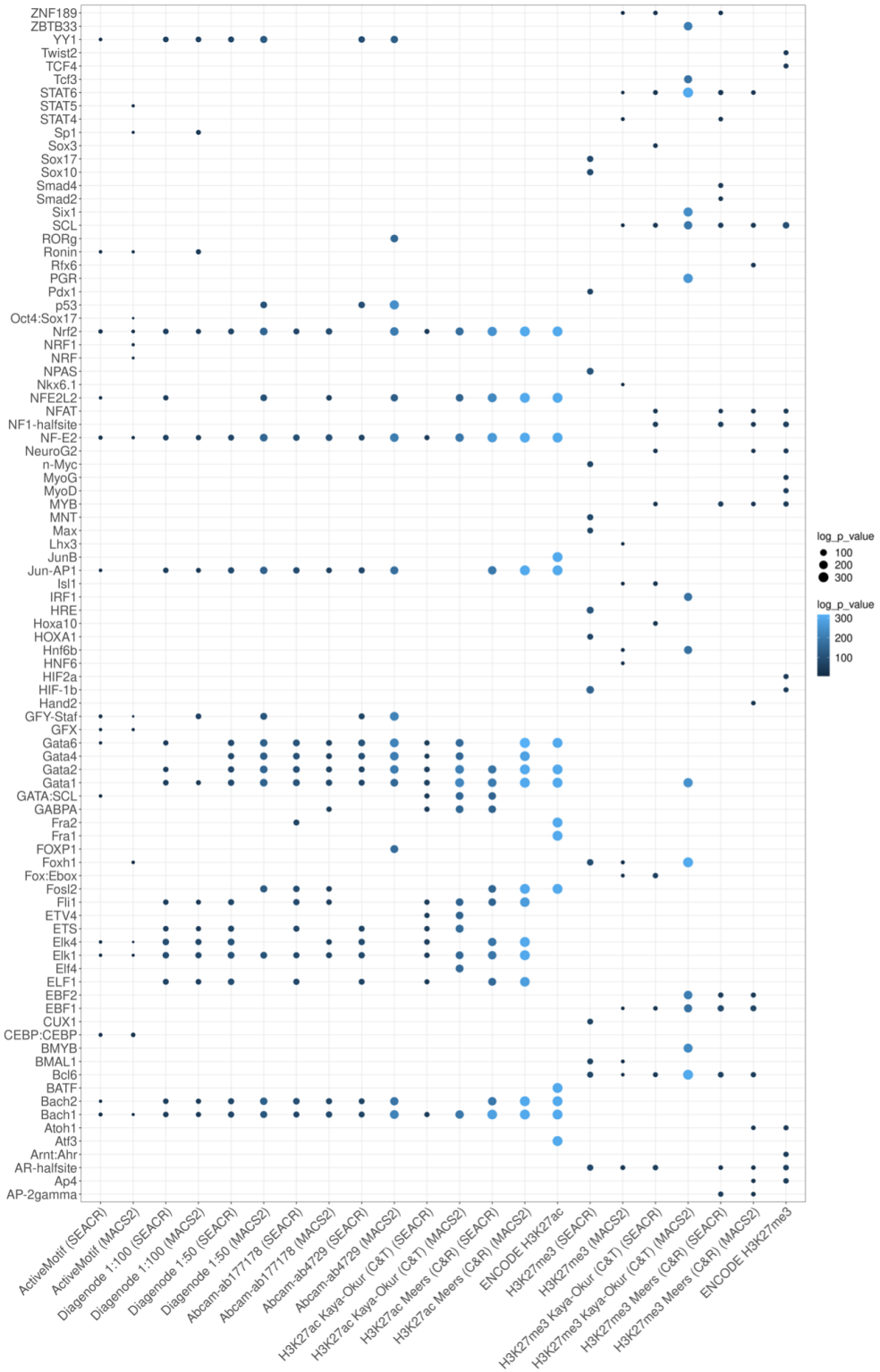

Supplementary Figure 7. Results of transcription factor binding motif (TFBM) enrichment analysis, showing the union of top 15 detected motifs for each sample. Expanded to include all tested samples and published datasets, with peaks called using both SEACR and MACS2.